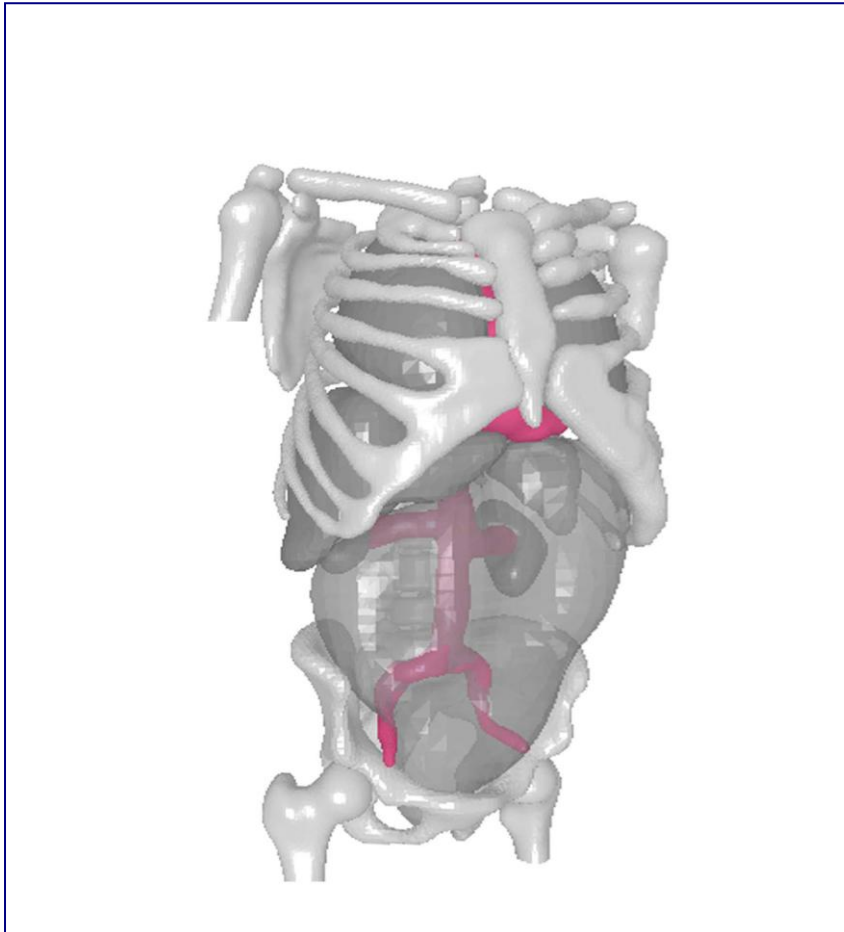# CHALMERS

Anthropometric Characterization of Human Subjects

Master's Thesis in the ERASMUS programme

MARTA GONZÁLEZ CARCEDO

Department of Applied Mechanics
Division of Vehicle Safety
CHALMERS UNIVERSITY OF TECHNOLOGY
Göteborg, Sweden 2010
Master's Thesis 2010:53

Anthropometric Characterization of Human Subjects

Master's Thesis in the ERASMUS programme

MARTA GONZÁLEZ CARCEDO

Department of Applied Mechanics
Division of Vehicle Safety
CHALMERS UNIVERSITY OF TECHNOLOGY
Göteborg, Sweden 2010

Anthropometric Characterization of Human Subjects
Master's Thesis in the ERASMUS programme
MARTA GONZÁLEZ CARCEDO

Cover:
Three dimensional surface model of skeleton and internal organs of subject 457.

Master's Thesis in the ERASMUS programme
MARTA GONZÁLEZ CARCEDO
Department of Applied Mechanics
Division of Vehicle Safety
Chalmers University of Technology

ABSTRACT

One of the factors that make development of protection systems complex is the human diversity. There is a significant spread in the size and shape of the population. In this master thesis project, the upper body of three post mortem human subjects with different sizes and shapes were selected to create mathematical models.

Based on computed tomography images of the subjects in supine posture and a software for performing analysis of medical images, three dimensional surface models were generated. Geometrical reconstruction of the skin, bones and internal organs was realized and then finite element models were meshed.

Lastly, the exterior (skin) and interior geometries (skeleton and internal organs) were extracted to characterize the size and shape. In addition the relationships between the external and internal measure were analysed.

Key words: Characterization human, computed tomography, finite element models, three dimensional surface models, anthropometry, post mortem human subjects.

II

Contents

IV

Preface

In this Master Thesis project the upper body geometries of a number of Post Mortem Human Subject (PHMS) were extracted. Three subjects were selected with different sizes and weights. And their geometries were reconstructed based on computed tomography scan data to create finite element models. An analysis of anthropometric characteristics was performed. The work has been carried out from March 2010 to September 2010 at the Division of Vehicle Safety, Department of Applied Mechanics, Chalmers University of Technology, Sweden, with Marta González Carcedo as student, Krystoffer Mroz as supervisor and Assistant Professor Karin Brolin as examiner.

I would also like to thank Autoliv AB Research and SAFER for their co-operation and involvement.

Göteborg September 2010

Marta González Carcedo

VI

1 Introduction

The analysis of restraint system designs that protect the vehicle occupants in a crash can be made through simulation with digital human models in virtual environments, as well as by the empirical and analytical methods. Within the realm of passive safety, widespread implementation of modelling into the design and evaluation process provides a viable means of achieving significant reductions in injury and fatality.

One of the factors that make development of protection systems complex is the human diversity that the systems need to protect. There is a significant spread in the size and weight of the population. In addition, the higher risk of injury for the obese or overweight occupant may be due to a combination of weight and its distribution, which alters the occupant's interaction with the vehicle interior and restraint system.

One of the main tools used in the development of the restraint systems are mechanical anthropometric test devices (crash dummies), which are also available as mathematical models. However, crash dummies are a crude representation of a human. A more recent tool that is starting to be commonly used is a detailed mathematical model of humans. The geometry of such human model is usually based on measurements of single Post Mortem Human Subject (PMHS).

Using medical imaging techniques, such as Computed Tomography (CT) scan data from PHMS, three dimensional surface models can be generated using digital geometry process with a large series of two dimensional X-ray images. It can provide three dimensional reconstructions of the human body including detailed soft tissues and internal organs.

The aim of this project is to create human body Finite Element (FE) models based on CT-scan data and to extract the main anthropometric dimensions from PHMS, with various size and shape. Focus is on the upper body, torso and abdomen, and the external and internal anthropometry.

2 Background

A brief description of human anatomy, injuries in the vehicle crash and medical imaging techniques are given below.

2.1 Anatomy and injuries

Several studies show the importance of injuries of the thorax and abdomen, identified as an area of high risk in traffic accidents. This importance is determined by several factors, one is the large number of injuries of the ribs. NASS data reveals that approximately 61% of all ASI2+ chest injuries are rib fracture.

The upper body takes a special importance in the design of prevention systems to protect vehicle occupants, including seat belts and airbags. In the Figure 2.1, Figure 2.2 risk and Figure 2.3 show risk of injury to different body regions for frontal, near-side and far-side crashes, evaluating for the main body regions. The head, the abdomen and thorax region are the highest level of injury presented in the different impacts.
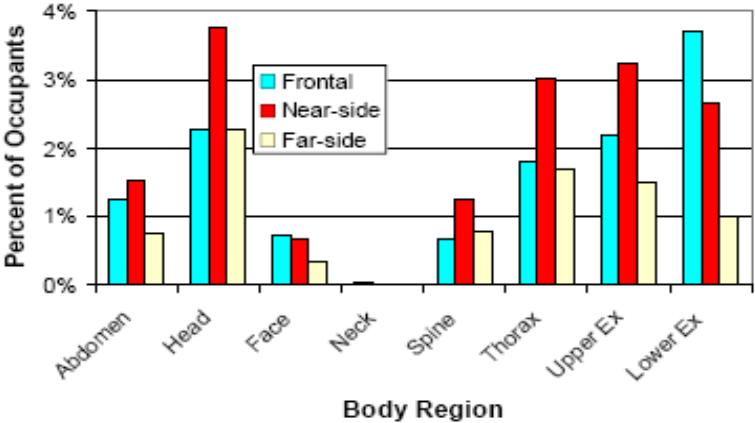

Figure 2.1: Risk of AIS 2+ injury by body region for frontal, near-side, and far-side impacts [Klinich et al.(2008)].
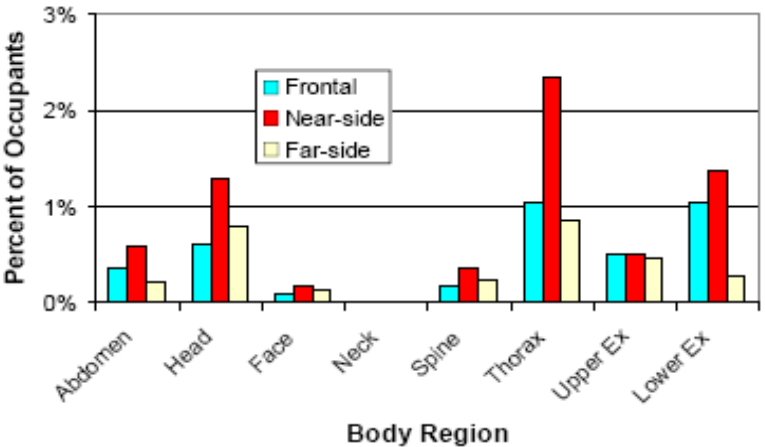

Figure 2.2: Risk of AIS 3+ injury by body region for frontal, near-side, and far- side impacts [Klinich et al.(2008)]
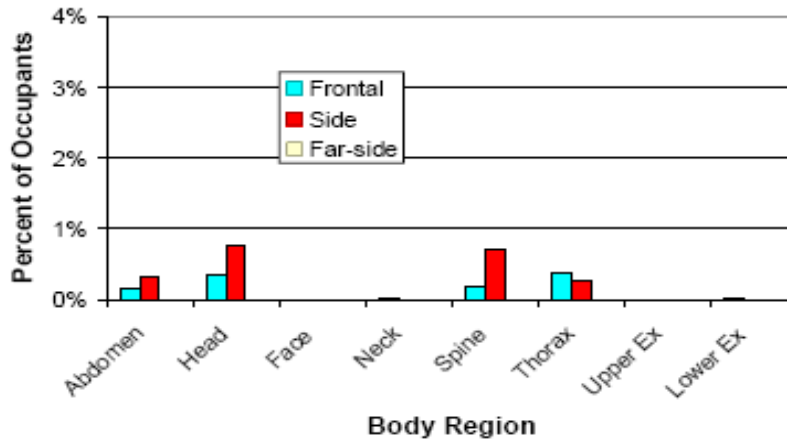
Figure 2.3: Risk of AIS 4+ injury by body region for frontal, near-side, and far-side impacts. [Klinich et al.(2008)].

The thorax is the second most frequently injured body region in traffic accident. In the thorax, there are several organs that when injured can cause serious injury or death. There is a relatively stiff part, consisting of the bony thorax with the ribs, sternum, clavicle, scapula or cervical spine. And another area consists in organs as heart, lungs, liver, kidney, aorta and others main arteries, which are weaker structures.

The abdomen is considered the third most frequently injured body region. In the abdomen, there are organs as stomach, intestine and spleen. Some organs are large and filled with blood as the liver, kidneys and spleen. The liver has 27% of the total blood flow, kidneys 22% and the spleen 5%, so one injury concern is haemorrhage.

2.2 Imaging technology

There are various modalities commonly in use today in medical imaging, two of them are Computed Tomography (CT) and Magnetic Resonance Imaging (MRI). These methods are used to create a digital geometry. Computer processing is used to generate a three-dimensional image of the human body from a large series of two-dimensional images.

CT image is ideal to use for scanning when the objects have different density, depending on absorption coefficient. However, CT image is not efficient at distinguishing between different soft tissues, the image quality will be poor. And MRI allows the excellent soft-tissue contrast. So CT and MRI are sensitive to different tissue properties, the appearance of the images obtained with the two techniques differ markedly.

2.2.1 Computed tomography

CT software processes a large volume of data to create two-dimensional cross-sectional images of the body. Pixels in an image obtained by CT scanning are displayed in terms of relative radio density, example in Figure 2.4.

At each sampling point within the volume, each type of scanner will measure a value relating the density of the material at that point which is converted into a pixel greyscale value. The

measurement relates to the amount of X-rays absorbed by the object. Organ with different density will get different pixel values. In this way, the different organs, tissues or volumes can be defined.
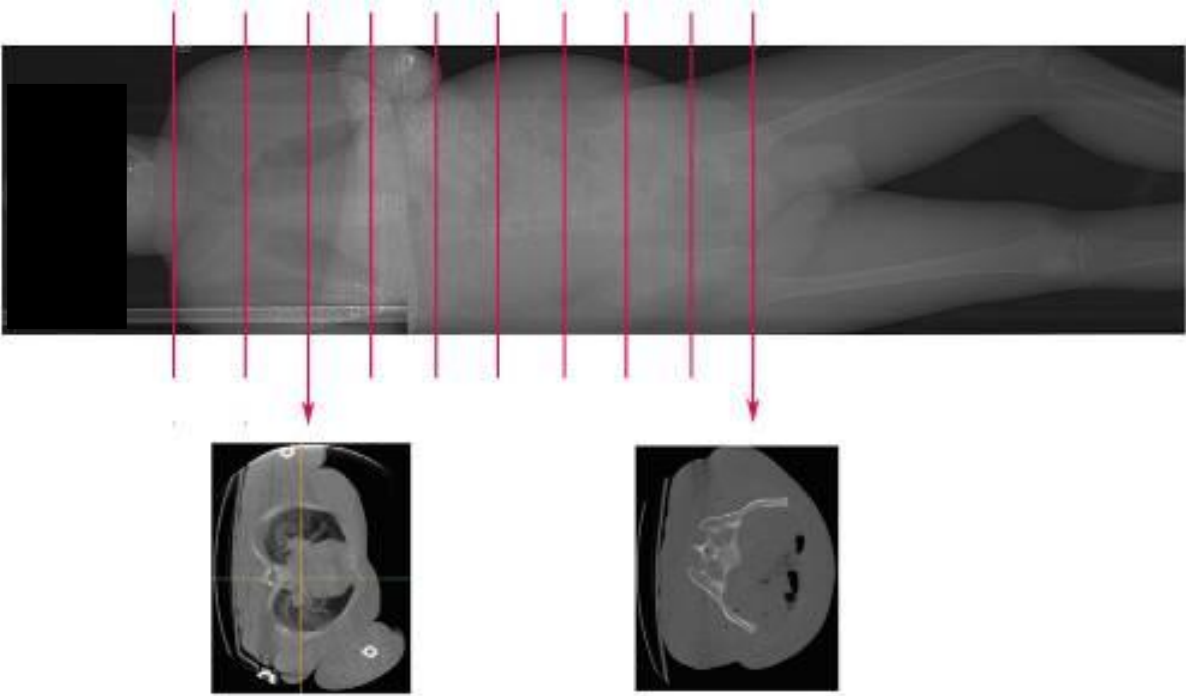

Figure 2.4: Image of CT [Forman J., Lessley D., Kent R. (2009)].

3 Method

Based on the literature review a methodology is defined, which involves PMHS data, software that process CT data and creation of surface models. In this section a description of the above stated along with the anatomy of interest is given.

3.1 Post mortem human subjects

The focus is on the upper body, torso and abdomen organs between the first thoracic vertebrae (T1) and the pelvis, focusing on the ribcage. The Table 3.1 defines different parts that will be modelled, differentiate between three groups: skeleton, organs and skin. The main joints shall be included such as the leg and arm joints.

Table 3.1: Specific parts for creation of 3D geometry.

PART NAME		
Skeleton	Thorax	Vertebrae (Thoracic T1-T12)
		Left ribs
		Right ribs
		Left scapula
		Right scapula
		Sternum
		Left clavicle
		Right clavicle
	Pelvis	Pelvis
		Sacrum
		Vertebrae (Lumbar L1-L5)
	Joint Positions	Join legs
		Join arms
Organs	Thorax	Heart
		Aorta
		Left Lung
		Right Lung
		Liver
		Left kidney
		Right kidney
	Abdomen	Spleen
		Intestine and bladder
Skin		

Three PMHS with various sizes are selected between several subjects to create the models. CT data of these subjects are from the University of Virginia, Centre for Applied Biomechanics, where the subjects were tested in several crash tests (NHTSA, 2008).
- Specimen ID: F- 437-A-08, with test number 1384.
- Specimen ID: M-457-A-08, with test number 1389.
- Specimen ID: M-404-A-07, with test number 1332.

A subject with very low body mass index is a female, and she is 54 years and her stature and weight are 247 cm. and 27.2 Kg. There is not a subject male with such a low weight and height as PHMS F437. So it is selected, it will take account in the evaluation that it is a female. The next subject is a male with 72 years and his stature and weight are 183 cm and 72 kg respectively. This subject has the characteristic mass and stature close to the average adult male. Lastly, a subject with a high body mass index is a male with 54 years and his stature is 189 cm. and weight is 124 Kg. Also their characteristics are shown in Table 3.2, defining Body Mass Index (BMI) as the weight in kilograms divided by the square of the height in meters (kg/m2). The BMI of the subject M404 is higher than 34.7, the World Health Organization (WHO) defines overweight as a BMI equal to or more than 25.

In addition in the Table 3.3 is shown other anthropometric measures of subjects taken by University of Virginia of these three subjects.

Table 3.2: Subject General Information. [Forman J., Lessley D., Kent R. (2008a,2008b,2009)].

PMHS #	Mass (Kg).	Stature (cm.)	BMI	Age	Gender
F437A08	27.2	147	12.6	54	Female
M457A08	73	175	23.8	72	Male
M404A07	124	189	34.7	54	Male

Table 3.3 Subject anthropometry information [Forman J., Lessley D., Kent R. (2008a,2008b,2009)].

Dimension	F437	M404	M457
	(cm unless otherwise noted)		
Sitting height	119.5	139.2	121
Shoulder (acromial) height	129.5	162	152
Shoulder width (bi-acromial)	32	43	39.7
Thoracic auxiliary width (4th rib)	23.4	40	32.9
Thoracic auxiliary thickness (4th rib)	17.5	23.5	23.3
Thoracic axilliary circumference (4th rib)	71	110.7	98.5
Thoracic sub-sternal width (8th rib)	24	36	32.5
Thoracic sub-sternal thickness (8th rib)	14	25.5	23
Thoracic sub-sternal circumference (8th rib)	64	114.3	96.7
Abdominal width	94.5	42.8	33.8
Abdominal thickness	14.5	28.1	18.5
Abdominal circumference	55.5	120	87
Pelvic (Iliac bi-crest) width	27	39.1	33.6
Pelvic depth	15.7	23.5	18.5
Pelvic circumference	68.8	118	93.4

3.1.1 Computed tomography scan data

The data used are CT-Scan in DICOM (Digital Imaging and Communications in Medicine) format with a resolution (width/height) of 512x512 pixels. Each individual was scanned in a number of series, with a specified number of images, pixel spacing and slice thickness. The subjects are in supine posture. There are two CT data sets of the whole body, the scans were made at different times.

Depending on the pixel spacing and slice thickness the image quality will vary. If the image quality is higher, the picture has more detail. Figure 3.1 shows two pictures with different dimensions of the pixel.
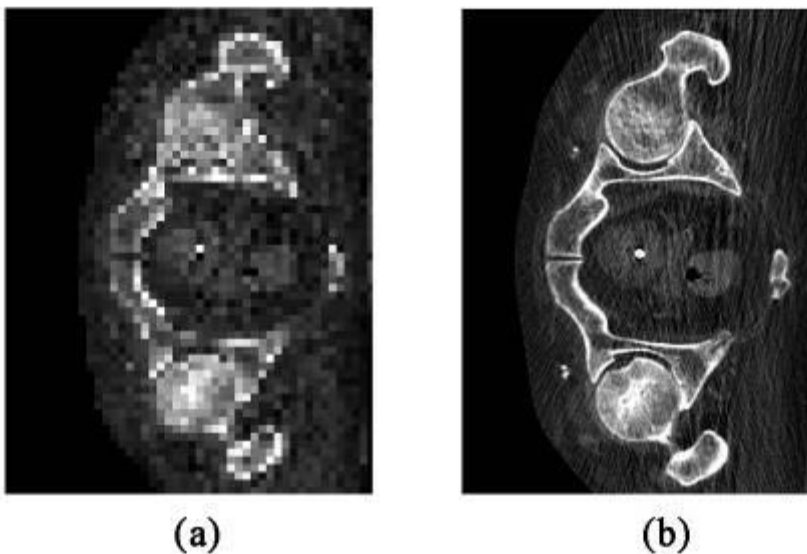
Figure 3.1: Different pixel size. We can see the different quality between two images, figure (a) the pixel size is 0.5x0.5 (mm.) while the image (b) the pixel size is 0.97x0.97 (mm). [Forman J., Lessley D., Kent R. (2009)].

Special filters or algorithms were applied in the scanning process, resulting in more detail in bones and lungs data. According to these characteristics the data of our subjects is analysed.

The data used in the project is that of before the crash test, except for subject F437. For F437 CT scan data after the first crash test is used since the data before crash test does not have enough data to model the upper body.

For the individual F437 reads two series. Series one and two have a pixel spacing of 0.97x0.97mm and slice thickness 0.62 mm, which is very low. The series two was used bone algorithm, to improve bone pixels. The images are of the whole body. This data is showed in the Table 3.4.

For the individual M457 reads eight series. Series one, two and six belong to an image of the surface of the individual, which we will use to define the outline of the individual. It has a pixel spacing of 0.5x0.5 mm. Series three, four, seven and eight have a pixel spacing of 0.97x0.97mm and slice thickness 0.62 mm. Series five has slice thickness 5 mm. Series three, four and five are images of the upper body and seven and eight series are images of the lower

body. And series four and eight were used with bone algorithm. This data of subject M457 is showed in the Table 3.5.

For the individual M404 reads seven series. Series one and four, with only two images belong to an image of the surface of the individual, which defines the outline of the individual. It has a pixel spacing of 0.54x0.59mm. Series two, three, six and seven have a pixel spacing of 0.97x0.97 mm. and 5 mm slice thickness. Series three is images of the upper body and the seven series are images of the lower body. The same applies to the series two and six but these are applied an algorithm which would improve the quality of the image according to the bone. And the series five, an algorithm is applied to define the lungs, also has a pixel spacing of less than 0.64x0.64 but only represents the thorax of the lungs. This data of subject M404 is showed in Table 3.6.

Table 3.4: Information about subjects M437 CT-scan data

Series No	Images	Part	Algorithm	Pixel Spacing (mm.)	Slice Thickness (mm.)
1	1330	Whole body	Standard	0.97/0.97	0.625
2	1330	Whole body	Bone	0.97/0.97	0.625

Table 3.5: Information about subjects M457 CT-scan data

Series No	Images	Part	Algorithm	Pixel Spacing (mm.)	Slice Thickness (mm.)
1	1	Whole body lateral	Standard	0.54/0.54	
2	2	Whole body frontal	Standard	0.54/0.54	
3	1434	Upper body	Standard	0.97/0.97	0.6
4	1434	Upper body	Bone	0.97/0.97	0.6
5	180	Upper body	Standard	0.97/0.97	5
6	2	Whole body lateral and frontal	Standard	0.54/0.54	
7	1889	Lower limb	Standard	0.97/0.97	0.6
8	1889	Lower limb	Bone	0.97/0.97	0.6

Table 3.6: Information about subjects M404 CT-scan data

Series No	Images	Part	Algorithm	Pixel Spacing (mm.)	Slice Thickness (mm.)
1	2	Lower body	Standard	0.54/0.59	
2	273	Lower body	Bone	0.97/0.97	5
3	273	Lower body	Standard	0.97/0.97	5
4	2	Upper body	Standard	0.54/0.59	
5	55	Upper body	Lung	0.64/0.64	5
6	121	Upper body	Bone	0.97/0.97	5
7	121	Upper body	Standard	0.97/0.97	5

3.2 Software that process computed tomography data

The data is processed with digital geometries methods. In this section includes an evaluation of different software.

3.2.1 Review of software

Based on a literature review several software that can be used to process DICOM data to produce FE models are evaluated. Defined a method based in the basic functions: pre-processing, segmentation and create masks, create the mesh, evaluate and export the finite element model, see Figure 3.2.

In the pre-processing a certain level of noise in the data which can be filtering, also the data can be reduced. The segmentation is the process where the different organs and bones are identified inside the slices. The pictures are separated into different parts depending on the pixel gray value levels of the CT scan images. After the model is meshed and exported the mesh.
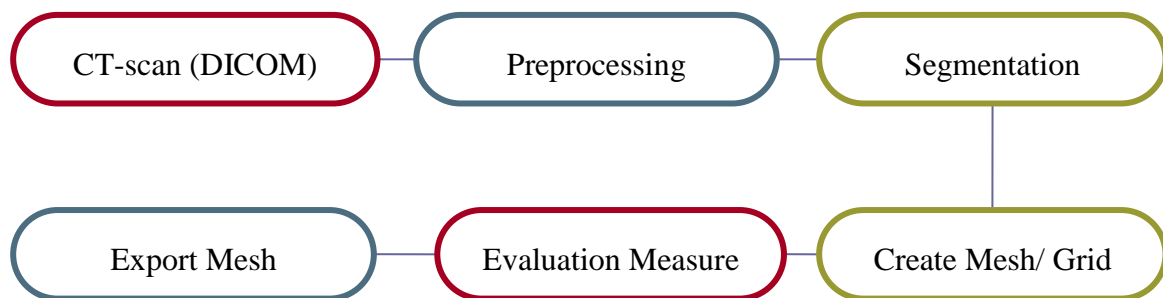

Figure 3.2: Functions required of software that can process CT data from DICOM format.

Based on the basic functions several software packages, available for performing analysis of medical images are evaluated. The following software packages were identified in this project, for performing analysis of the medical images:

- MIMICS (Tutorial Guide Materialise: MIMICS (2010)).
- SIMPLEWARE: ScanIP/ScanFE (Simpleware Reference Guide (2010)).
- Amira (Tutorial Guide AMIRA (2010)).
- 3D-Slicer: IA-Mesh/ Free Surfer (Tutorial Guide of 3D Slicer(2010), Tutorial Guide IA-FEMesh, Tutorial Guide of FreeSurfer).
- Slicer Dicer (Guide SlicerDicer (2010)).
- MicroDICOM (Tutorial Guide of MicroDicom).
- Gemldent (Tutorial Guide of GemIdent (2006))
- ITK-VTK (Tutorial Guide of ITK –VTK).
- ImageJ-FIJI (Tutorial Guide of ImageJ).

3.2.2 Evaluation of software

The following steps are used to evaluate four software selected to choose a software to create the three dimensional models.

- Type of license evaluating: the cost and time.
- Tools that offers, interface and interaction with the program.
- Time necessary between actions.
- Problems and limitations.
- Support, manuals and examples tutorials.

And also some part or parts, some bone or organ of a subject will be modelled with each program.

3.3 Creation of surface models

This process can be divided into several main stages: the slicing procedure (preparation data and filtering, Section 3.4.1), identification of the organs on the slices (segmentation and create masks, Section 3.4.2), 3D reconstruction and validation of the data (evaluation contact surface, Section 3.4.3) and a final stage of creation mesh (Section 3.4.4).

### 3.3.1 Import, data preparation and filtering

Using Simpleware Scan IP, DICOM files are imported, the number of the series is chosen and the data is prepared reducing the noise. Also, crop and resample is very useful for the large datasets. On some occasions re-align is necessary, thus creating a new set of slices (In PHMS M457 and M404), see Figure 3.3. Additionally there are several data sets of the whole body that need to align.
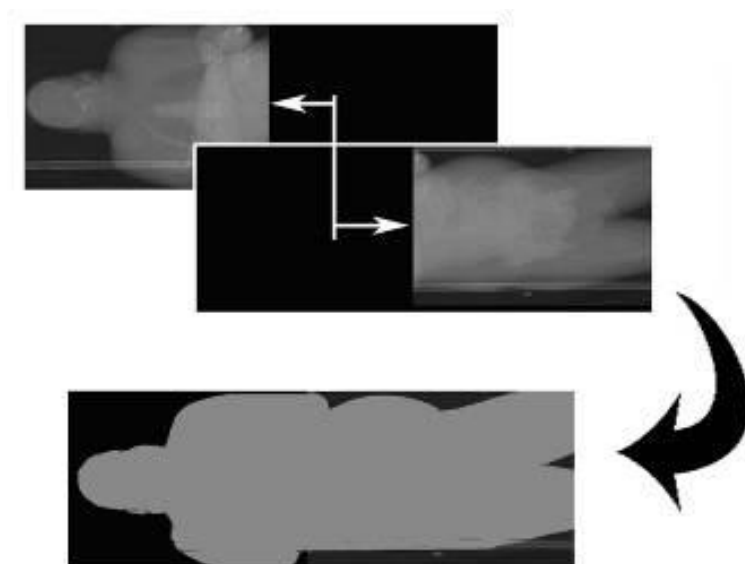
Figure 3.3: Example of image alignment. We have different images and we have to rotate and translate to align to get a new image. [Forman J., Lessley D., Kent R. (2009].

3.3.2 Segmentation

It is the process of identifying which object each pixel belongs to. The segmentation applies to differences CT images, separating the images into different parts depending of the pixel value into gray levels of the CT scan images. Most of the time to model generation process is spent on segmentation, because is the process of identifying which object each pixel belongs to. Each organ have different density, so the organ or soft tissue is defined depending on pixel values, see example Figure 3.4. Each pixel creates a voxel, and the volume images can be considered as three dimensional tables containing intensity values for particular positions in space. To delimit the structures, we can use semiautomatic methods or manual methods when the contrast between the different parts is not clear.
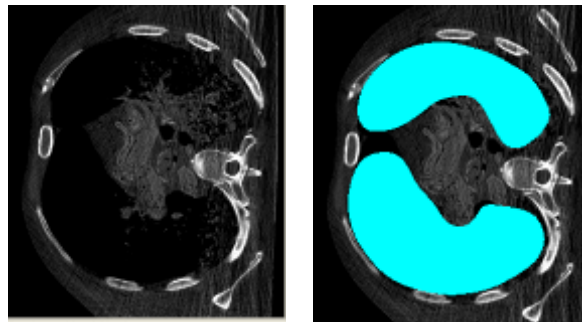

Figure 3.4: Example of segmentation of the lungs from PMHS M457. [Forman J., Lessley D., Kent R. (2009)].

In addition these masks can be worked on; the software offers a wide range of filters for different applications. Two commonly used categories of filter are smoothing and noise reducing. Smoothing reduce of noise but also attenuate contours. The second one, noise reducing filters, reduces noise while preserving features as much as possible. Also Boolean operations are used, applying intersections or unions, invert or subtract between masks.

Incorrect use of the filters causes the loss of characteristics of the shape and size of our organs or parts that has been modelled. The filter and number of iterations depend on each form and dimensions of the organ or bone. See Figure 3.5, example of evaluation of vertebrae L3 of the PHMS M457, which applies the filter Smoothing-Recursive Gaussian with different parameters. For the same organ is applied the same parameters and filter for the three models, for comparison.

After creating the different parts, the contact surfaces are evaluated. Making sure that these are in correct position and dimensions, checking these do not use spaces of their neighbours.
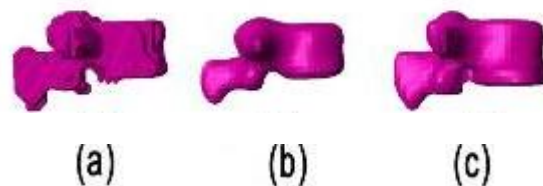
Figure 3.5: Example of application filters: Smoothing – Recursive Gaussian Filter. Vertebrae L3 of PHMS 457wich is applied different parameters in the filter Smoothing-Recursive Gaussian: In the model (a) is applied a low parameter and inadequate for this model,

contrary in the model (b) is applied a high parameter and same volume and details of the shape is lost. The model (c)is a suitable smoothening. So, with high or low value of smooth the model loses volume and details in the shape

3.3.3 Mesh generation and export.

Once the data is ready and all the masks are segmented and evaluated, models were created based on the masks. Thereafter finite elements models are created, which can export as shells (surface elements) or volumes.

Choosing the option to export as a volume for the evaluation to calculate the centre of gravity of the parts (depends on the mass). And for the skin is better use shell elements that reduce the number of model elements. So shell elements for the skin, and the others models solid and shells elements.

The pixel voxels are converted in surfaces creating a mesh. In which the dimensions of the model mesh are defined, depends on the size and shape. Each part organ or bone has been defined a size of element. The organs have different sizes and shapes. For each organ was evaluated and defined the most appropriate element size. In Figure 3.6 the real form is compared of the rib of Subject M457, evaluating for different elements size.
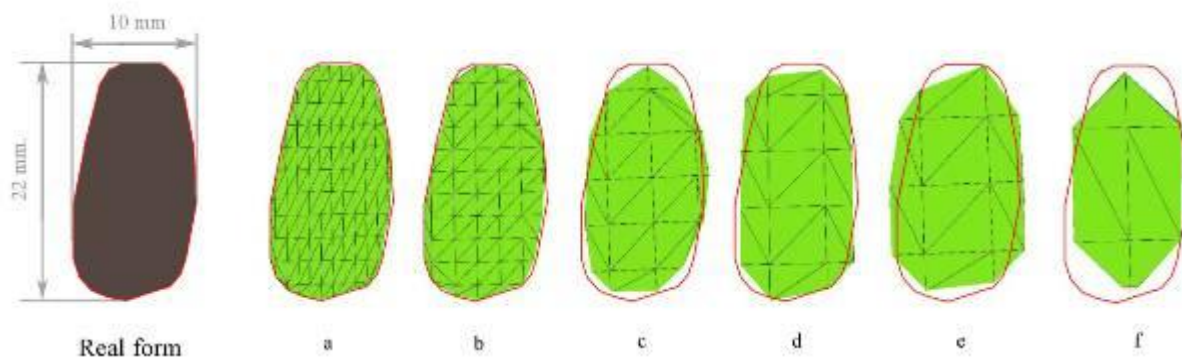
	Real Form	a	b	c	d	e	f
Mesh size (mm.)	0.97x0.97x5	1x1x2	2x2x2	4x4x4	6x6x6	8x8x8	10x10x10
Number of elements	100 %	142.6%	55.7%	13.5%	6.6%	3.4%	2.1%
Reduce or increase number of elements	100%	42.6% Inc.	44.36% Red.	86.5% Red.	93.9% Red.	96.6% Red.	97.9% Red.

Figure 3.6: Evaluation elements size mesh of a rib of PHMS M457.

In addition to evaluate graphically the size of the mesh, are evaluated numerically, evaluating how change the mesh size on the number of elements. According their volume, Figure 3.7 the mesh size is compared with the volume of the model. The form most closely to the real figure will *model (b).* This elements size of the mesh is defined for the ribs.
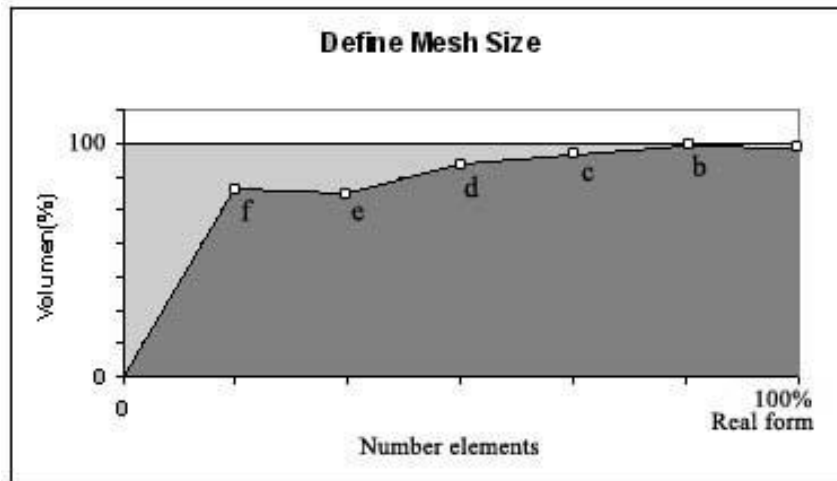
Figure 3.7: Define mesh size based volume model, according Figure 3.6.

### 3.3.4 Extracting anthropometric dimensions

The anthropometric dimensions are extracted from the three 3D models, according with Figure 3.8. To characterize the external size and shape of the specimens, anthropometric dimensions were extracted from the three 3D models.

With the software LS-PrePost (LS-PrePost Tutorial Guide (2010)) the anthropometric dimensions are extracted from the three 3D models. The dimensions of body mass, height in standing position and sitting height are extracted of the report NHTSA (Forman J., Lessley D., Kent R. (2008a,2008b,2009)).

- Body Mass [Kg].
- Height in standing position [m].
- Sitting height [m] Seated between head to buttock.
- Shoulder (acromial) height [m].
- Shoulder width (bi-acromial), including and excluding soft tissue [m].
- Thoracic axillaries width (4th rib), including and excluding soft tissue [m].
- Thoracic axillaries thickness (4th rib), including and excluding soft tissue [m].
- Thoracic axilliary circumference (4th rib), including and excluding soft tissue [m].
- Thoracic sub-sternal width (8th rib), including and excluding soft tissue [m].
- Thoracic sub-sterna thickness (8th rib), including and excluding soft tissue [m].
- Thoracic sub-sterna circumference (8th rib), including and excluding soft tissue [m].
- Abdominal width [m].
- Abdominal thickness [m].
- Abdominal circumference [m].
- Pelvic (Iliac bi-crest) width, including and excluding soft tissue [m].
- Pelvic depth, including and excluding soft tissue [m].
- Pelvic circumference, including soft tissue [m].

And the measures are extracted for the internal organs are:

- Area [m^2].
- Volume [m^3].
- Center gravite (x,y,z) [m].
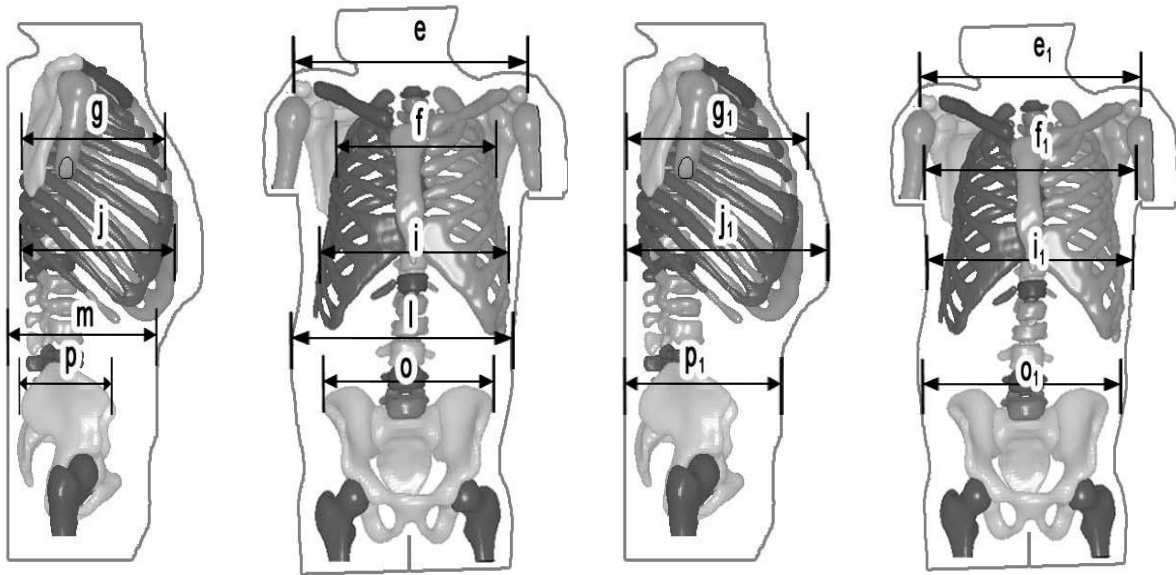
(e). Shoulder width (bi-acromial), including and excluding soft tissue [m]
(f). Thoracic axillary width (4th rib), including soft tissue [m]
(g). Thoracic axillaries thickness (4th rib), including soft tissue [m]
(i). Thoracic sub-sterna width (8th rib), including soft tissue [m]
(j). Thoracic sub-sterna thickness (8th rib), including soft tissue [m]
(l). Abdominal width [m].
(m). Abdominal thickness [m]
(0). Pelvic (Iliac bi-crest) width, including soft tissue [m].
(p). Pelvic depth, including soft tissue [m]

(e_1). Shoulder width (bi-acromial), excluding and excluding soft tissue [m]
(f_1). Thoracic axillaries width (4th rib), excluding soft tissue [m]
(g_1). Thoracic axillaries thickness (4th rib), excluding soft tissue [m]
(i_1). Thoracic sub-sternal width (8th rib), excluding soft tissue [m]
(j_1). Thoracic sub-sternal thickness (8th rib), excluding soft tissue [m]
(0_1). Pelvic (Iliac bi-crest) width, excluding soft tissue [m].
(p_1). Pelvic depth, excluding soft tissue [m]

Figure 3.8: Anthropometric measurements

3.3.5 Anthropometric dimensions

The anthropometric measures are extracted and the data subject was from the report NHTSA [Forman J., Lessley D., Kent R. (2008a,2008b,2009)].

The thoracic axillaries in 4th rib, was taken approximately at the midpoint of the rib four, through the longitudinal plane of the model (plane z), so created a line belong to the plane transverse to the model between midpoint of the rib four right and midpoint rib four left. The same for the thoracic axillaries in 8th rib, was taken approximately at the midpoint of the rib eight, see Figure 3.9

For the thoracic axilliary circumference in the 4th rib, measure is taken in a transverse plane and that include two points the midpoint of the rib four and the midpoint of the seven thoracic

vertebrae. And the same for the thoracic axilliary circumference in the 8th rib, measure is taken in a transverse plane and that include two points the midpoint of the rib eight and the midpoint of the eleven thoracic vertebrae. Both planes are roughly parallel, see Figure 3.10.
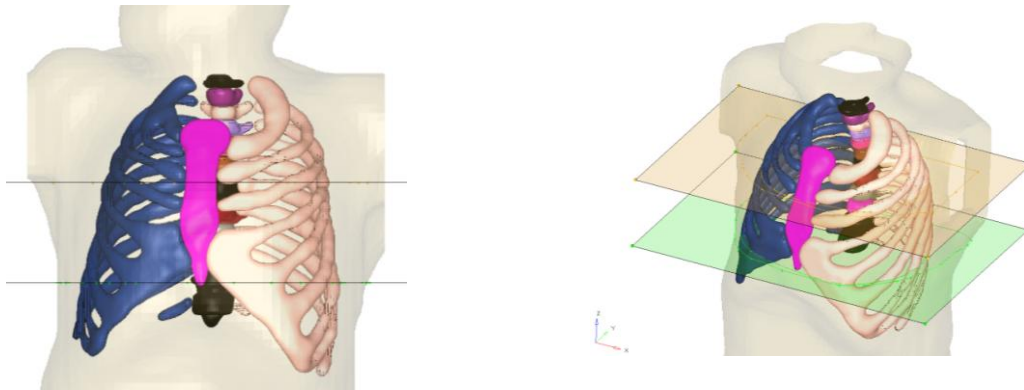
Figure 3.9: Explanation about the measure of the thoracic axillaries: First line measure of the thoracic axillaries 4th rib and the second line thoracic axillaries 8 th rib.

Figure 3.10: Three dimensions view of the planes to take the measure of the thoracic axilliary circumference.

The points of the model which are close of the plane are reflected, through its points a line approximately the circumference is drawn and the longitude of this circumference is extracted. These measures were taken a including and excluding soft tissue. When it is excluded soft tissue, is created the line of the rib cage, excluding the scapula (only taken into account ribs, vertebrae and sternum). The Model 457 the thoracic auxiliary circumference in the 4th rib including the soft tissue, is the same high than the arms, so the circumference approximately is drawn trying excluding the arms.

4 Results

Following the methodology, the results are obtained according to CT-scan data, evaluation of software, creation models and analyses of anthropometric dimensions.

4.1 Post mortem human subjects

The figures below are shown through the different parts that are modelled. The upper body skeleton, including skeleton, skin and internal organs. The skeleton consisting of: clavicle, scapula, rib cages, sacrum, pelvis, sternum and dorsal spine, see Figure 4.1. The dorsal spine is differentiated in lumbar vertebrae (five vertebrae, L1 to L5) and thoracic vertebrae (twelve vertebrae, T1 to T12). The internal organs consisting of: lungs, heart, spleen, kidneys, liver, aorta, intestine and bladder, see Figure 4.2. The intestine and bladder are modelling together. Stomach cannot be modelled, because of the quality of the images.
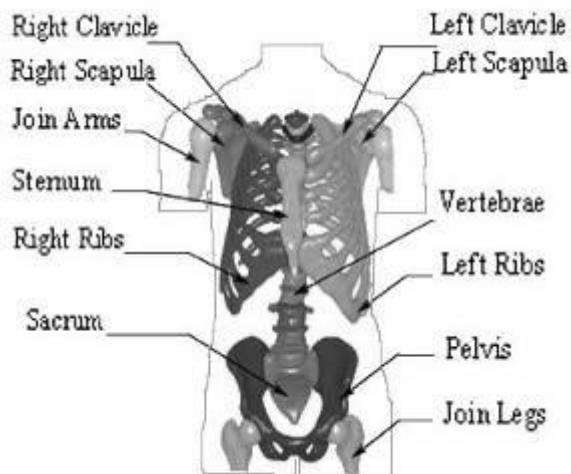
Figure 4.1: Image of upper body skeleton.
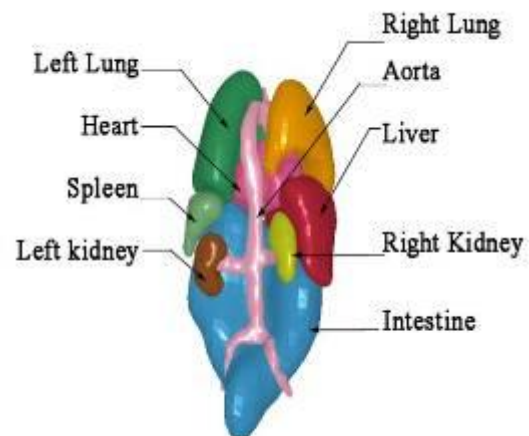
Figure 4.2: Image of upper body organs.

In Table 4.1 is defined different parts were modelled. In the three subject individuals are able to model the skeleton and can differentiate between the different bones. In addition, each vertebra (five lumbar vertebrae and twelve thoracic vertebrae) were modelled as an independent parts. The skin could be defined in the three subjects.

Organs as heart, lungs, aorta, intestine and bladder could be modelled in the three subjects. Could not be possible to model some of the others organs of the quality of the images.

Table 4.1: Parts for creation of 3D geometry.

PART NAME			F437	M404	M457
Skeleton	Thorax	Vertebrae (Thoracic T1-T12)	✓	✓	✓
		Left ribs	✓	✓	✓
		Right ribs	✓	✓	✓
		Left scapula	✓	✓	✓
		Right scapula	✓	✓	✓
		Sternum	✓	✓	✓
		Left clavicle	✓	✓	✓
		Right clavicle	✓	✓	✓
	Pelvis	Pelvis	✓	✓	✓
		Sacrum	✓	✓	✓
		Vertebrae (Lumbar L1-L5)	✓	✓	✓
	Joint Positions	Join legs	✓	✓	✓
		Join arms	✓	✓	✓
Organs	Thorax	Heart	✓	✓	✓
		Aorta	✓	✓	✓
		Left Lung	✓	✓	✓
		Right Lung	✓	✓	✓
		Liver	✗	✓	✓
		Left kidney	✗	✓	✓
		Right kidney	✗	✓	✓
	Abdomen	Spleen	✗	✓	✓
		Intestine and Bladder	✓	✓	✓
Skin			✓	✓	✓

The subject F437 the quality of the images is low and some organs could not be modelled: liver, kidney and spleen. In addition, as mentioned above, the images before crash test cannot be used, where some bones are broken, between vertebrae thoracic nine and vertebrae thoracic seven. So this vertebrae thoracic seven (T7), eight (T8) and nine (T9) are reconstructed and ribs seven and eight (back part).

Also some slices have problems, called "metal artefacts", it often appear when scanning metallic objects at the same time as organic subjects. It is not distort the geometry but it hide information. This phenomenon appears in same slice, in the lumbar vertebrae (L5) and ten thoracic vertebrae (T10), both vertebrae are reconstructed. (In the 3D model is able to see where are situated metals parts.)

The subject M404 was modelled using two background images together. The quality of the images is good. The subject M457 the quality of the images is very good, I can define the dimensions and the situation of the organs with detail.

4.2 Software that process computed tomography data

Based on the basic functions several software packages, available for performing analysis of medical images are evaluated. The Table 4.2 shows the different software that could be used. For this evaluation the trial version is used to test the software.

Table 4.2: Descriptions of the reviewed software

Name Program	Evaluation	Description
Mimics	✓	For a more extensible evaluation
Simpleware ScanIP / ScanFE	✓	
Amira	✓	
3D-Slicer (IA-mesh/Free Surfer)	✓	
Slicer Dicer	✗	It creates orthogonal and oblique slices, and projected it in a plane.
Microdicom	✗	It is for manipulation of DICOM images 2D. Not3D
Gemldent	✗	It is for identification regions and colours in images and photographs.
ITK - VTK	✗	It uses language C++, is complex.
ImageJ - FIJI	✗	Images processing is in 2D and 3D but it only process, does not create models.

Based on the basic functions, four programs are selected for a more extensive evaluation:

- MIMICS (Table 4.3),
- Simpleware (Table 4.4),
- Amira (Table 4.5),
- and 3D-Slicer (Table 4.6).

4.3 Evaluation of software

For this extensible evaluation four software are tested using their trial version for each software: MIMICS, Simpleware, Amira and 3D-Slicer.These software are testing, evaluating tools, limitation, supports and others parameters that are set for the evaluation (Section 3.3.2). In addition, a part or parts of the model M457, some bone or organ, are modelled with each program.

After extensible evaluation and comparison, the software chosen to create the 3D models is Simpleware ScanIP and Scan FE.

Table 4.3: Evaluation software MIMICS [Tutorial Guide Materialise: MIMICS (2010), Forman J., Lessley D., Kent R. (2009)].

MIMICS Materialise

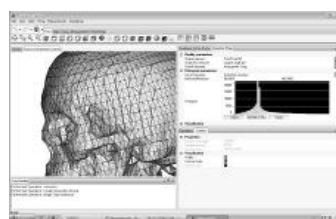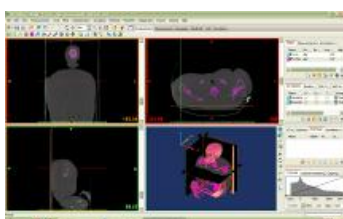|	
License	Base license. And modules: FEA module (finite element and CFD preparation), STL+ module (export module) A perpetual license or six months. Version student for 6 months. Expensive price.
Tools	PREPARING DATA: Histogram in the work screen, options to improve image quality: Cropping, size of the image is reduce, low memory. PREPROCESING: Reduce noise in the image: Gaussian filter, binomial, mean, median, others. Segmentation regions: semiautomatic with threshold, Boolean, cavity fill and morphology filters. And manual polylines 2D and 3D. CREATING a 3D preview model: connecting with regions. MEASURE: can take in 3D model or slices 2D. MESHING: remeshing and edit. EXPORT formats are: Patran, Ansys, Abaqus, Fluent, Nastran, Comsol.
Interface	Very good and easy the use. It has three slices windows and 3D view window.
Problems	In version student cannot export.
Used	It takes an average level of dedication to the program.
Support	Support in line, tutorial is not good, has not examples.

Table 4.4: Evaluation software Simpleware ScanIP/ScanFE. [Simpleware Reference Guide (2010), Forman J., Lessley D., Kent R. (2009)].

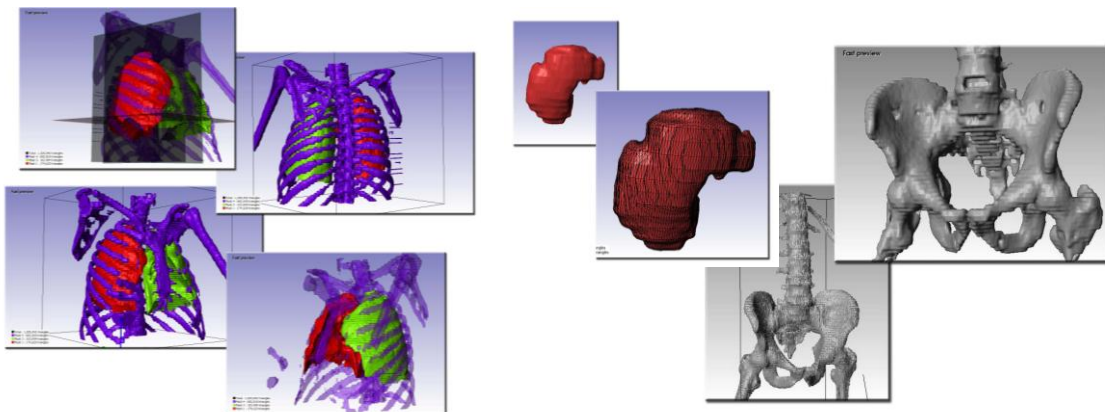|	SIMPLEWARE - Scan IP / Scan FE.
License	Academic for a year, for 6 months and 3 months. With modules: ScanIP/ScanFe/ ScanCAD. Intermedial price.
Tools	PREPARING DATA: Preview histogram when you import the data, options to improve image quality, also you have when you are working. When you export you can crop, reducing the size of the image, low memory. You can work with different files, use several background. PREPROCESING: Reduce noise in the image with filters: Gaussian, smoothing, cavity fill. Segmentation regions: semiautomatic with threshold and flood fill, and manuals. CREATING a 3D preview model: connecting with regions and post-smooth. MEASURE: can take in 3D model or slices 2D. MESHING: FEmesh generation, adjust and edit. Mesh refinement. EXPORT in ScanIP to ScanFE (to LSDYNA) solids or shells.
Interface	Medium level interaction with the program. Description: 3 slices view windows and other with the 3D model.
Problems	Memory limited, when you import the files (2 GB) and some problems when you work with big files. You cannot choose the number of elements but you can change the size elements.
Used	It takes an average level of dedication to the program. Medium easy used.
Support	It has very good and fast online support. Good tutorials with examples and problems.

Table 4.5: Evaluation software AMIRA. [Tutorial Guide AMIRA (2010), Forman J., Lessley D., Kent R. (2009)].

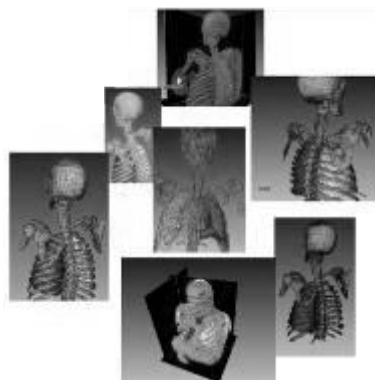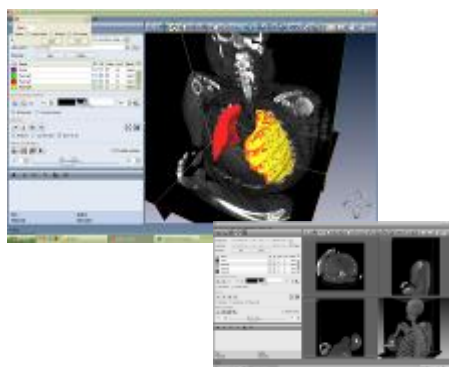| AMIRA.	
License	Base pack + Amira Dicom Reader. Expensive price.
Tools	PREPROCESING: Histogram in the screen where you work, Open different files in different times. Cropping, size of the image is reduce, low memory. Orthogonal slices, bounding box, isosurface, volume rendering (colour map, texture). SEGMENTATION: Label field: semiautomatic: Threshold and manual: brush. Filters: Gaussian filter, refine smoothing, remove islands and others. MEASURE: in the volume, material statics. Segmentation regions: semiautomatic with threshold and flood fill, and manuals methods. CREATING 3D: surface reconstruction from 3D images: Surface Gen: generate triangular surface. Grid generation. Simplify surface. Editing surface: surface view, surface editor. Test: edge flip, collapse, bisection. Post processing: Grid editor, generation tetrahedral grid- tretagen. Mesh size, gridvolumen. You can choose the number of elements. EXPORT with AMIRA Mesh option to HyperMesh.
Interface	Medium level interaction with the program. Description: Window with 3D model with the exception in the segmentation option that it has 3 windows + model.
Problems	Not undos/redos.
Used	Program has easy level of use. Medium easy used.
Support	It has very good online support, but it has not good tutorials.

Table 4.6Evaluation software 3D-Slicer. [Tutorial Guide of 3D Slicer(2010), Forman J., Lessley D., Kent R. (2009)].

3D SLICER	
License	Free version.
Tools	PREPROCESING: Segmentation regions with semiautomatic: threshold (but it is not good) and manual. It has not tools to delete unnecessary parts. It cuts image. It cannot open different files. CREATING a 3D model: it need a lot of time. MEASURE, MESHING and EXPORT: I could not do it. I can´t model any model properly.
Interface	Difficult understanding. It has 3 windows and the 3d view.
Problems	It needs a lot of time. Lot of stops and I have to start again. Cut image and it does not open same files. It cannot open several files (use different backgrounds at the same time).
Used	It takes a high level of dedication to the program. Difficult used.
Support	It has not good tutorials, without examples.
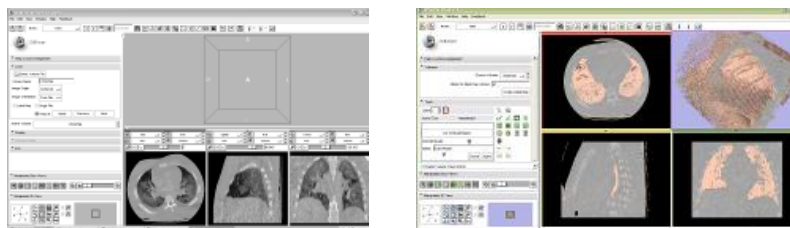
4.4 Creation of surface models

This section presents the results from the main steps: data preparation, segmentation, mesh generation and model assemble (Section 4.4.1 and 4.4.2). Also, the anthropometric dimension of the models are listed in Section 4.4.3.

4.4.1   Data preparation and segmentation

The organs of subject M457 could be modelled in great detail, the data has good quality. In contrast the subjects M404 and F437 their quality data are not as good, but the organs could be defined. Although the liver, spleen and kidney could not modelled in model F437.

The subject M404 is modelled using two background images together, but this causes any problem because the data was put together and aligned. Also the subject M404, some organs

as liver, kidney and aorta can differ with real dimensions, caused for the resolution of pixel (greyscale).

The quality of the data of subject F437 is low and some organs could not be modelled: liver, kidney and spleen. There are not enough data before crash test to model, so the data after crash test is used. By using this data, some bones were broken as vertebrae thoracic seven, eight and nine (T7, T8 and T9) and we have to reconstruct and also, the ribs seven and eight in the back part (part near to the spine).

The data of subject F437 had some difficulties to model some small parts, such as the ribs. The ribs were difficult define to smooth, for two reasons: one is the complexity of the ribs and small size (because the subject has a small ribcage), and the others it is the quality of the data. Also, the ribs are closely spaced from each other, this makes when it is modelled. There a fusion between some ribs because the slices thickness. And also the twelve ribs are missing. Some slices are affected by phenomenon "metal artefacts". This phenomenon hide data (it is explained in Section 4.2) and some vertebrae need to be reconstructed: lumbar vertebrae five (L5) and thoracic vertebrae ten (T10).

4.4.2 Mesh generation and assemble

When the model had been created with voxels, it is exported to ScanFE, where the voxels are converted into surfaces, creating a mesh. See Figure 4.3, where in the second picture we have a 3D model created with voxels, in the first picture the models is transformed in a mesh.
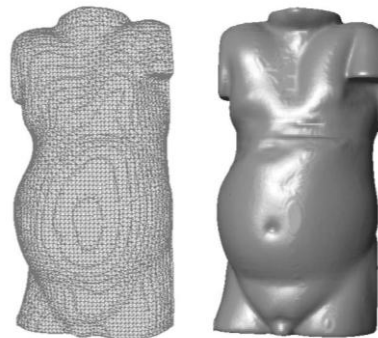
Figure 4.3: The voxels are converted in a surfaces, creating a mesh

Based in the shape and the real size of the organs and bones, a element mesh size is defined for each organ. The software Simpleware ScanIP or ScanFE is not allow the definitions of element size or number of elements. Changing the value pixel spacing, it reduces the number of element and size, also reduces the volume of data. So, three size are defined, depends on the dimensions and shape of the organs: small, medium and big size. Small elements mesh size for complex shapes and small parts: rib cage (vertebrae, ribs, clavicle, scapula, and sternum) and heart, aorta, kidney and spleen, applying pixel spacing cubic around 3 mm. It was impossible to create the models with smaller element size, because the volume of data is big and uses a lot of memory and the computer used cannot run. Other mesh size for the join parts legs and arms, pelvis, sacrum and liver, applying a pixel spacing cubic, around 5mm. And the big mesh size in the big parts: lungs, intestine (intestine and bladder together) and skin, applying resampling of the pixel spacing around 10 mm.

However this size does not mean it is the size of the elements of the mesh, it depends on the shape of the model. The models are created in ScanIP and exported to ScanFE to create and edit the mesh. And the last step is ensemble, the parts are exported in different models, each organ and each bone is a model and jointed with the software LS-PrePost to create the three dimensional models from the three subjects.

The models are grouped in skeleton, organs and skin. The skeleton is divided into the different bones differentiating between ribs, scapula, clavicle, sternum, pelvis and spine. And this are differentiating between their situated, ribs right and rib left, and the same with clavicle and scapula. About the spine, each vertebra is modelled separately distinguishing between lumbar and thoracic vertebrae, see Figure 4.4.

The organs are modelled individual each organ, differentiating between right and left organs in the case of lungs or kidney, see Figure 4.5. The results of assemble are three surface models of three subjects. See Figure 4.6, the models are divided in skeleton, internal organs and skin.

Figure 4.4: Three dimensional model of the skeleton (with different views) showing the spine in detail (differentiating each vertebra), from the model M457

Figure 4.5: Three dimensional model of the organs, showing details of the aorta and the kidneys, from the model M457

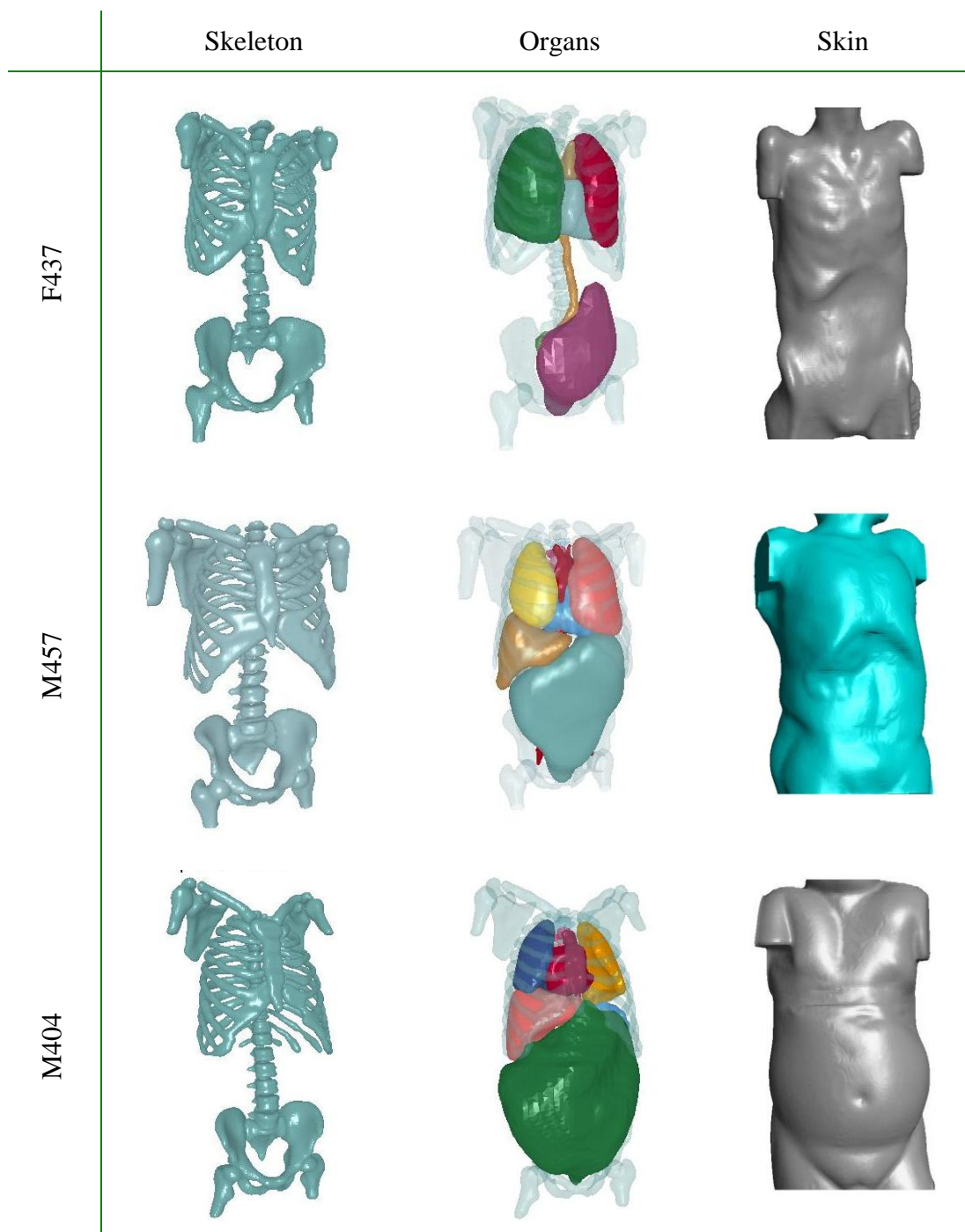|	Skeleton	Organs	Skin
F437			
M457			
M404			

Figure 4.6: Dimension models of skeleton, organs and skin from the three subjects..

4.4.3 Anthropometric dimensions

The thoracic axilliary circumference in 4th and 8th rib are extracted, see Figure 4.7. These measures were taken a including and excluding soft tissue. This soft tissue includes skin and fat layer.

The anthropometric dimensions extracted from the subjects are listed in Table 4.7, Table 4.8 and Table 4.9. These tables compare with experimentally measured dimensions of body mass, height in standing position and sitting height, which cannot be extracted from the 3D models, since only upper body was modelled.
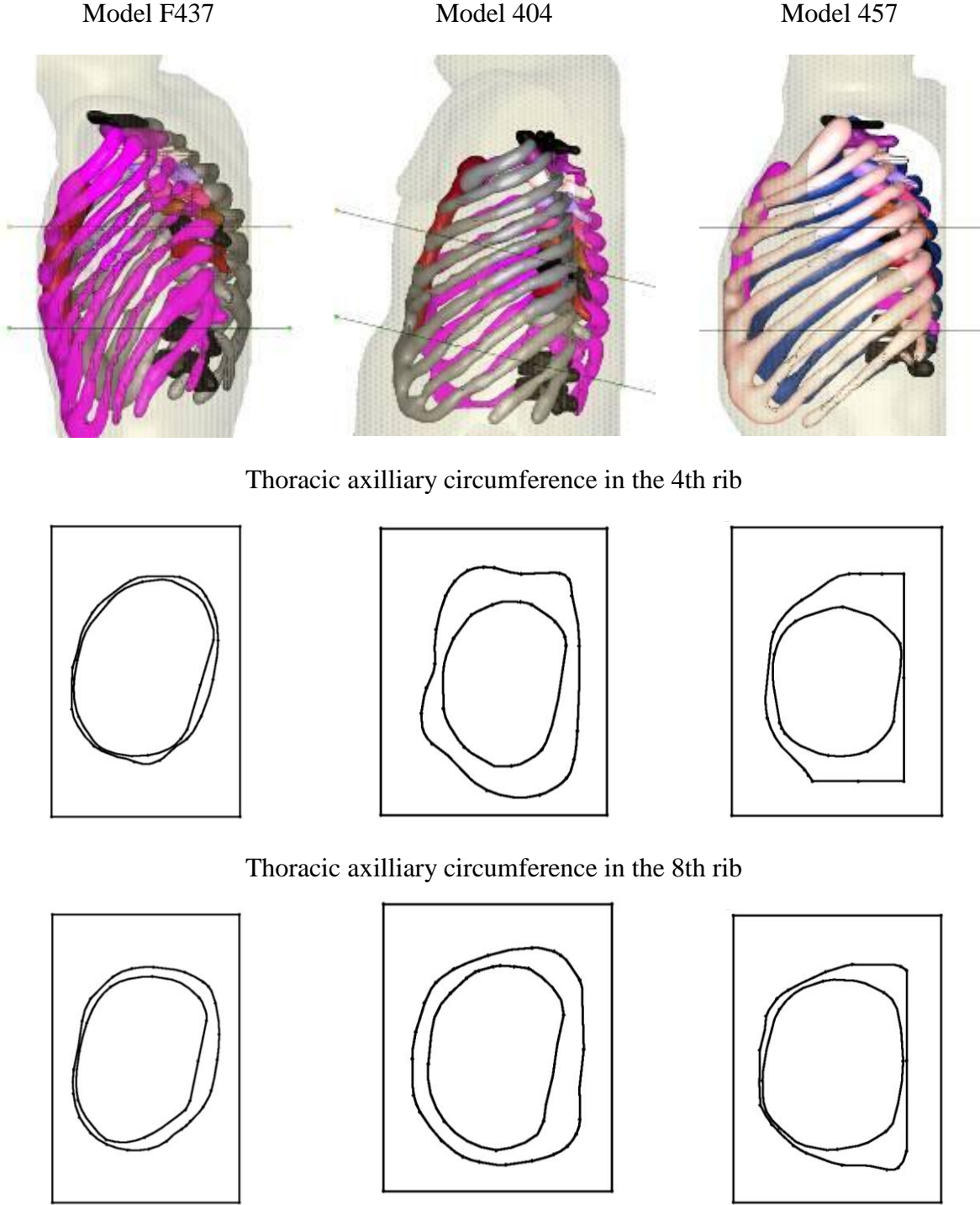

Figure 4.7: The thoracic axilliary circumference from the three models: showing the planes in the model and project the line created for the ribcage and the skin in both planes.

Table 4.7: Main anthropometry dimensions model F437. The data subject was extracted of the report NHTSA [Forman J., Lessley D., Kent R. (2008a,2008b,2009)]

| Dimension | Unit | Data Subject | Data 3D-Models | |
			Excluding soft tissue	Including soft tissue
Body Mass	kg	27.2		
Height (in standing position)	cm	147		
Sitting height	cm	82		
Shoulder (acromial) height	cm	129.5		
Shoulder width (bi-acromial)	cm	32	28	31
Thoracic axillary width (4th rib)	cm	23.4	22.6	24
Thoracic axillary thickness (4th rib)	cm	17.5	15.6	18
Thoracic axilliary circumference (4th rib)	cm	71	65.9	73
Thoracic sub-sternal width (8th rib)	cm	24	24.4	26
Thoracic sub-sternal thickness (8th rib)	cm	14	14	15
Thoracic sub-sternal circumference (8th rib)	cm	64	69	73.6
Abdominal width	cm	94.5	✘	24.5
Abdominal thickness	cm	14.5	✘	14.5
Pelvic (Iliac bi-crest) width	cm	27	250	26
Pelvic depth	cm	15.7	123	15

Table 4.8: Main anthropometry dimensions model M404. The data subject was extracted of the report NHTSA [Forman J., Lessley D., Kent R. (2008a,2008b,2009)]

| Dimension | Unit | Data Subject | Data 3D-Models | |
			Excluding soft tissue	Including soft tissue
Body Mass (Kg.)	Kg	124		
Height (in standing position)	cm	189		
Sitting height	cm	98		
Shoulder (acromial) height	cm	162		
Shoulder width (bi-acromial)	cm	43	35	42
Thoracic axillary width (4th rib)	cm	40	25	40
Thoracic axillary thickness (4th rib)	cm	23.5	17	24
Thoracic axilliary circumference (4th rib)	cm	110.7	81.7	115.7
Thoracic sub-sternal width (8th rib)	cm	36	31	36
Thoracic sub-sternal thickness (8th rib)	cm	25.5	23	26
Thoracic sub-sternal circumference (8th rib)	cm	114.3	90.7	113.5
Abdominal width	cm	42.8	✘	42
Abdominal thickness	cm	28.1	✘	30
Pelvic (Iliac bi-crest) width	cm	39.1	26	39
Pelvic depth	cm	23.5	12	27

Table 4.9: Main anthropometry dimensions model M457. The data subject was extracted of the report NHTSA [Forman J., Lessley D., Kent R. (2008a,2008b,2009)]

Dimension	Unit	Data Subject	Data 3D-Models Excluding soft tissue	Including soft tissue
Body Mass (Kg.)	Kg	73		
Height (in standing position)	cm	175		
Sitting height	cm	89		
Shoulder (acromial) height	cm	152		
Shoulder width (bi-acromial)	cm	39.7	36.2	40
Thoracic axillary width (4th rib)	cm	32.9	26	34
Thoracic axillary thickness (4th rib)	cm	23.3	20	23.1
Thoracic axilliary circumference (4th rib)	cm	98.5	77.6	106.6
Thoracic sub-sternal width (8th rib)	cm	32.5	29.6	34
Thoracic sub-sternal thickness (8th rib)	cm	23	23	24
Thoracic sub-sternal circumference (8th rib)	cm	96.7	88.4	106.4
Abdominal width	cm	33.8	✖	34.8
Abdominal thickness	cm	18.5	✖	19
Pelvic (Iliac bi-crest) width	cm	33.6	26.4	34
Pelvic depth	cm	18.5	16	18.1

And the measures are extracted for the internal organs are: area, volume and centre of gravity to characterize the shape and size of the organs. The measures are extracted from the three 3D models, see Table 4.10, Table 4.11 and Table 4.12 are showed. To calculate the center of gravity, a homogeneous specific density was assumed for all solid organs.

Table 4.10: Dimension internal organs 3D model F437

ORGANS	Area (cm^2)	Volume (cm^3)	Centre of gravity (cm) X	y	z
Heart	658.6	278.4	17.5	6.9	40.8
Aorta	658.6	101.7	17.6	9.1	40.5
Left Lung	1822.7	1005.6	22.4	7.7	43.7
Right Lung	2155.6	1450.9	11.1	10.2	44.8
Liver	✖	✖	✖	✖	✖
Left kidney	✖	✖	✖	✖	✖
Right kidney	✖	✖	✖	✖	✖
Spleen	✖	✖	✖	✖	✖
Intestine and bladder	1726.5	1041.3	16.9	8.7	14.3

Table 4.11: Dimension internal organs 3D model M404

ORGANS	Area (cm^2)	Volume (cm^3)	Centre of gravity (cm)		
			x	y	z
Heart	1429.1	765.5	22.8	17.8	64.4
Aorta	1072.6	184.6	24.3	19	48
Left Lung	2002.8	1095.2	32.2	20.6	65.5
Right Lung	2112.3	1236.9	16.6	22.5	66.5
Liver	2985.2	2089.7	15.5	21.1	54
Left kidney	530.9	178.4	31.7	17.7	44.4
Right kidney	487.5	147.3	14.4	20.9	41.5
Spleen	773.6	273	34.8	22.2	52
Intestine and bladder	8821.5	7864.1	20.9	12.5	36.8

Table 4.12: Dimension internal organs 3D model M457

ORGANS	Area (cm^2)	Volume (cm^3)	Centre of gravity (cm)		
			x	y	z
Heart	1387.7	606.1	28.4	12.1	49.4
Aorta	2036.7	389.7	21.2	15	37.4
Left Lung	1954.1	1073.7	28.4	12.1	49.4
Right Lung	2793.2	1696.6	15	13.4	52.1
Liver	2127.3	1279.9	12.2	14.4	38.7
Left kidney	550.2	150.8	28.6	18	30.6
Right kidney	495.9	138.2	14.1	20	34.4
Spleen	552.1	184.3	31.3	18	37.9
Intestine and bladder	5025.2	3978.4	21.3	12.3	25.2

4.5 Analyses of anthropometric dimensions

The three models are compared the external anthropometric measurements: body mass, height and sitting height, with the internal measurements organs. In the comparison the artery aorta is excluded, because it differs in the three models caused of the quality of the data. In a model M457 is defined in great detail and change in the other two model, the part of the abdomen lose some details, being difficult to define.

The body mass versus the volume of the internal organs Figure 4.8, where the size of the internal organs depends linearly with the size of the internal organs, increasing the size of the organs with the body mass, except right lung. The correlation coefficient for the heart is 0.95 for the left lung is 0.90, for the right lung is 0.25 and for the intestine and bladder is 0.87. The correlation coefficient of the others variables is not necessary because there is only data from two subject, and the coefficient in this case would be one.

The size of the internal organs depend linearly of the height. Increasing the size of the organs respect of the height, except the right lung, see Figure 4.9. The correlation coefficient for the heart is one. For the left lung is 0.99, for the right lung is 0.08 and for the intestine and

bladder is 0.93. Excepting the right lung, the values are very near than one. The size of the organs and height depends linearly.

The size of the internal organs is compared with the sitting height, see Figure 4.10. Increasing the size of the organs respect of the sitting height, except the right lung. The correlation coefficient for the heart is 0.94, for the left lung is 0.87, for the right lung is 0.28 and for the intestine and bladder is 0.99. The values are very close than one, so sitting height has a strong relation with the size of the organs.

Also, the volume of the internal organs depends of the BMI, see Figure 4.11. Increasing the size respect of the BMI, close than linear relationship, except right lung.

Comparing the measures were taken including and excluding soft tissue, the dimension of the layout of the soft tissue is analysed, see the Figure 4.12. The difference between the measures excluding and including is showed, the soft tissue in the area of the pelvic increase very fast respect others parts, the slope of line that draw the points is very high, instead in the thoracic sub-sternal (8th rib) the value of the slope in this case is very low, the increase is very small.

The external measures of the skin of the abdominal is compared with the body mass in the three subjects, see Figure 4.13. Showing in both direction thickness and width.
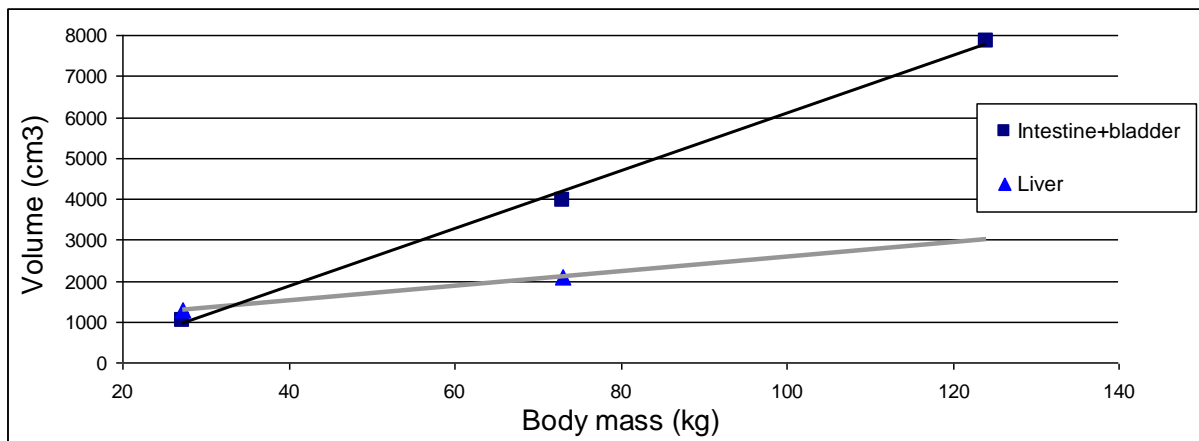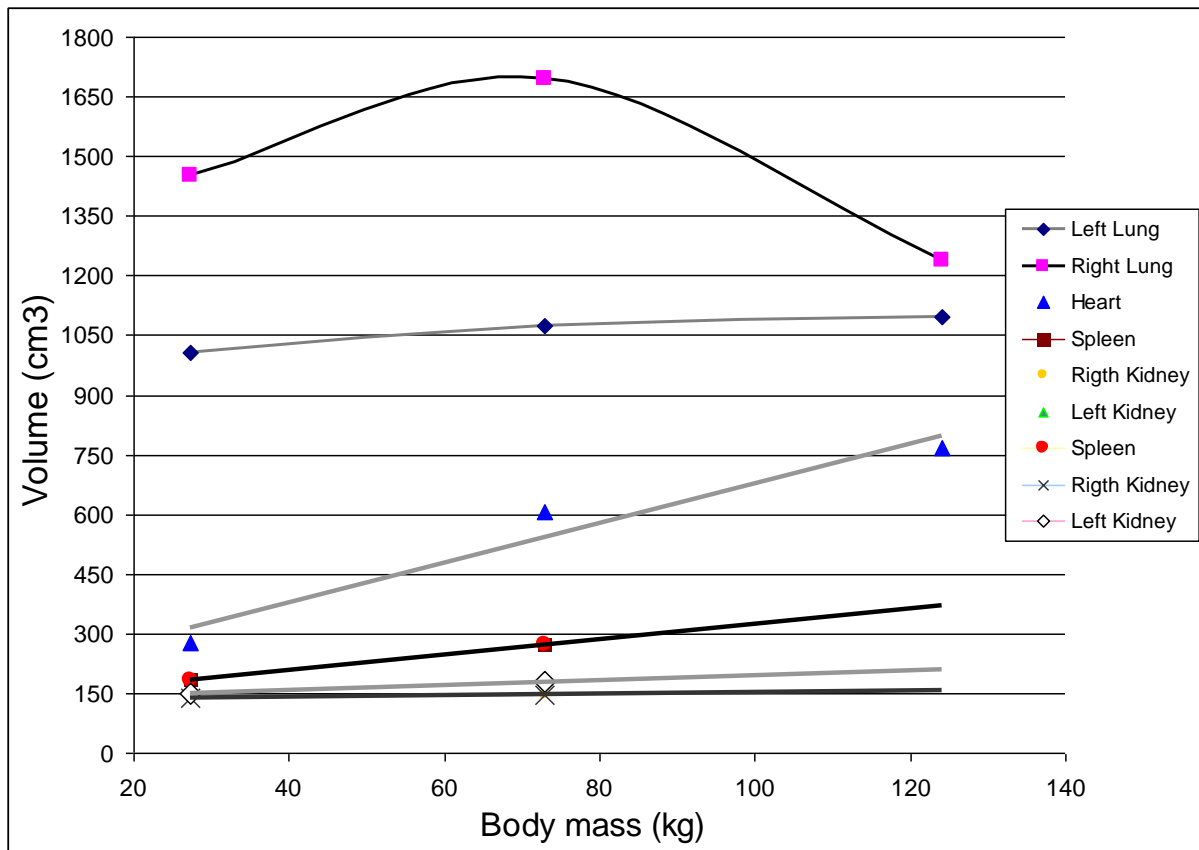
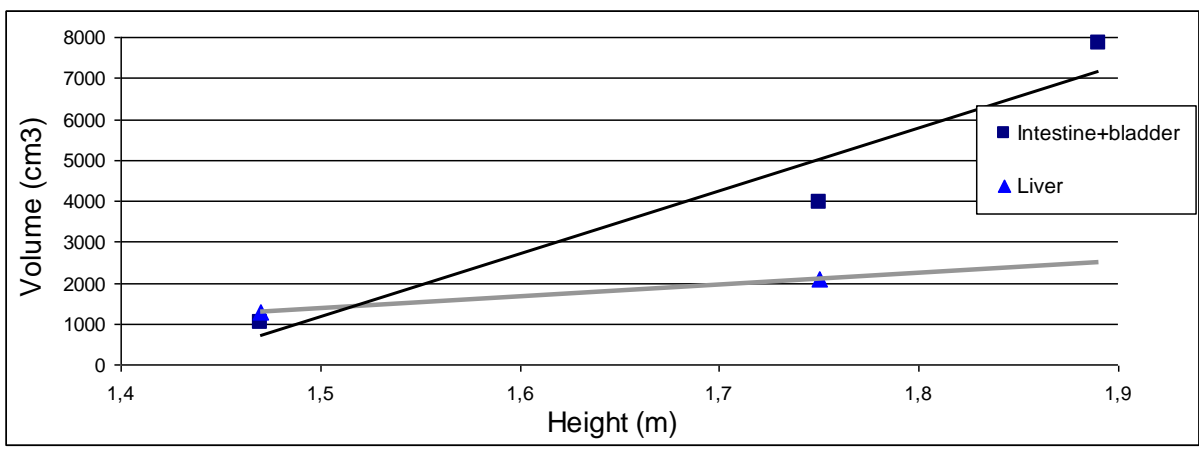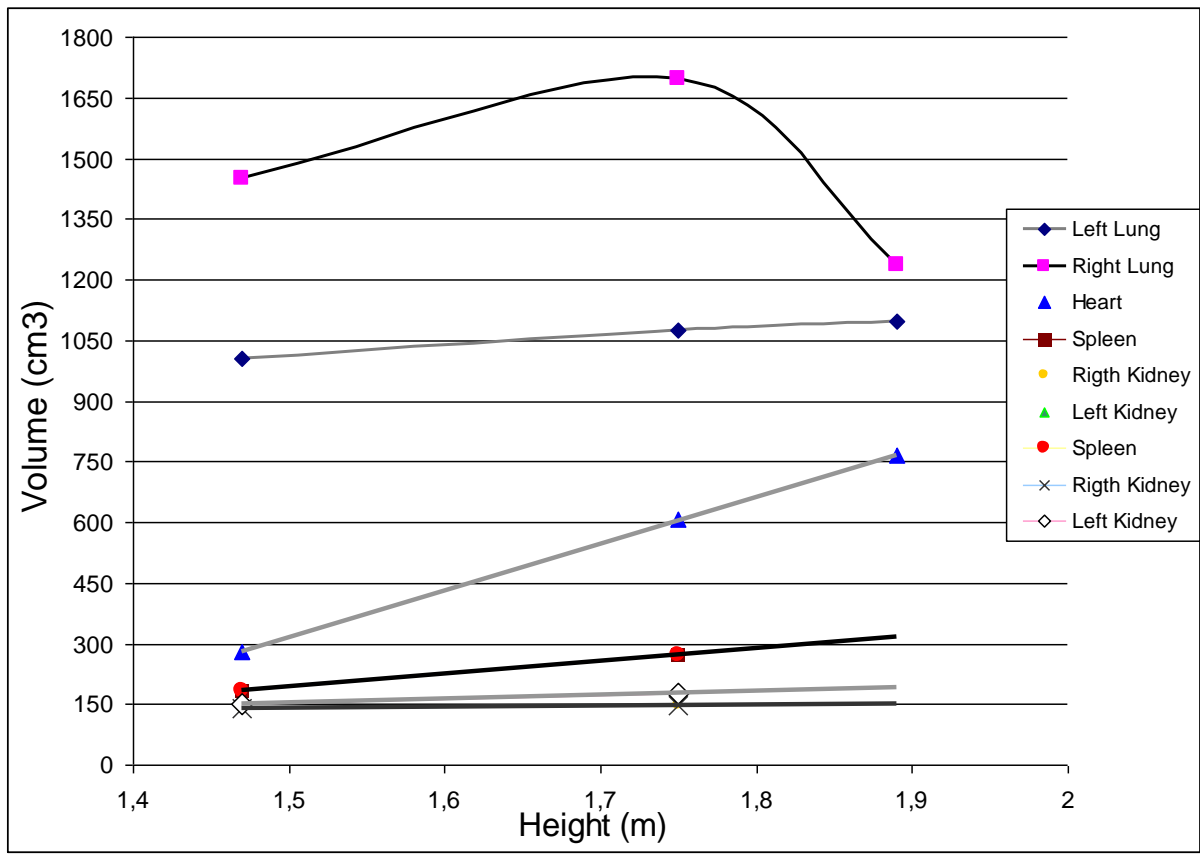*Figure 4.8: Body mass versus volume internal organs of the three models*

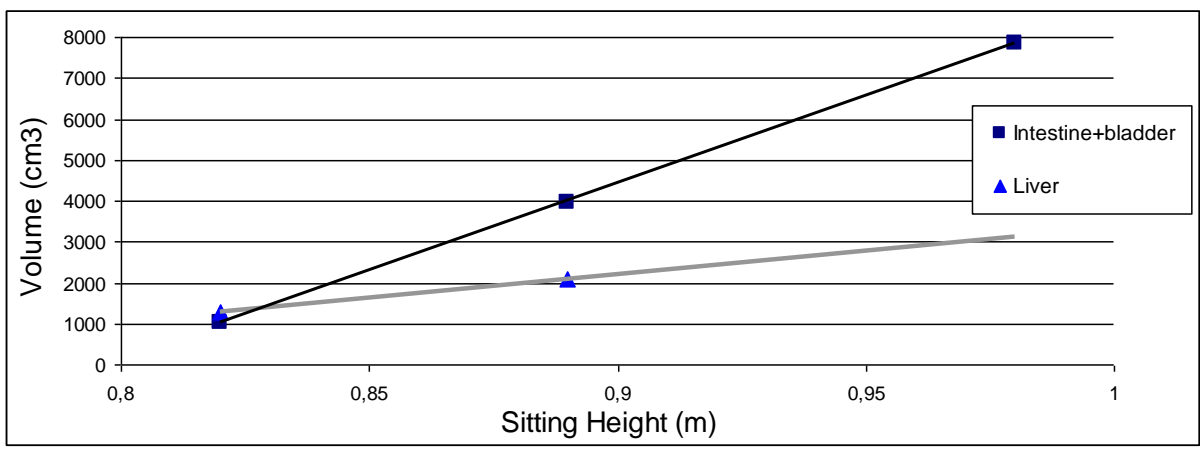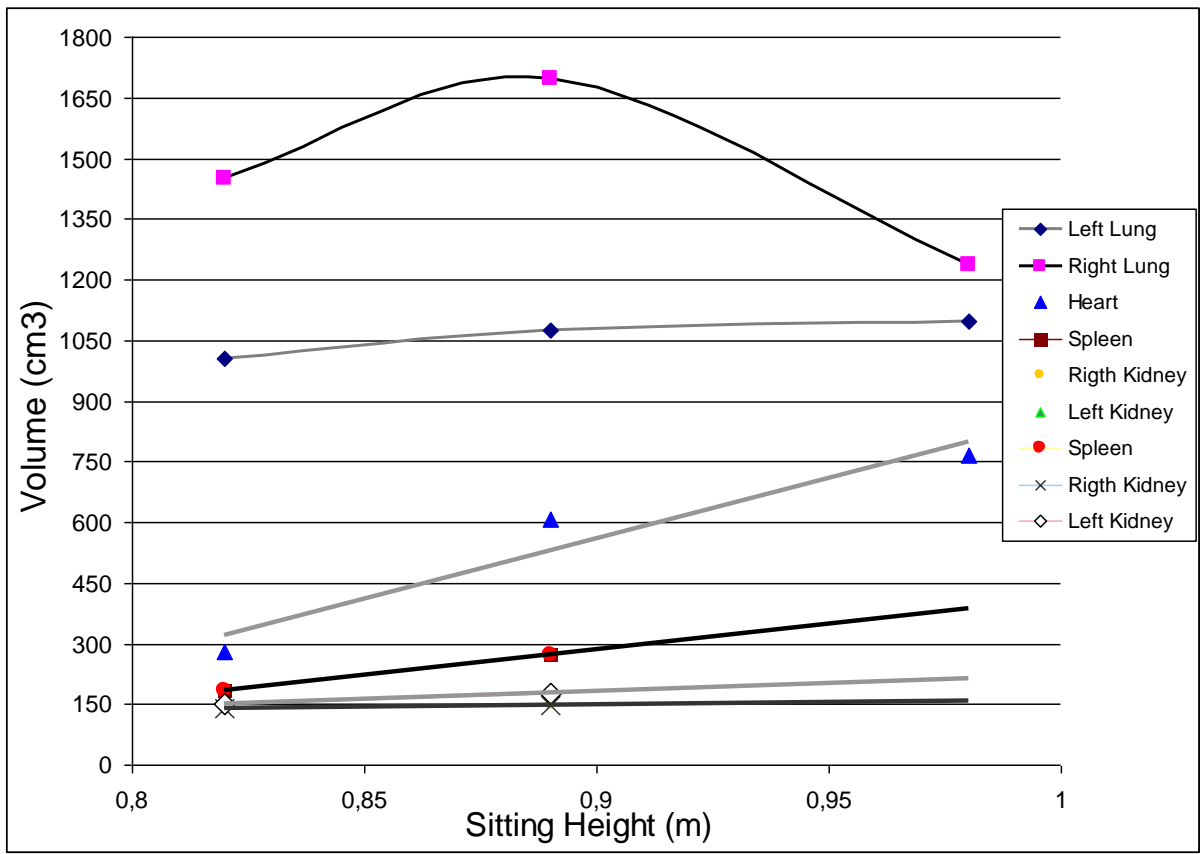*Figure 4.9: Height versus volume internal organs of the three models.*

Figure 4.10: Sitting height versus volume internal organs of the three models
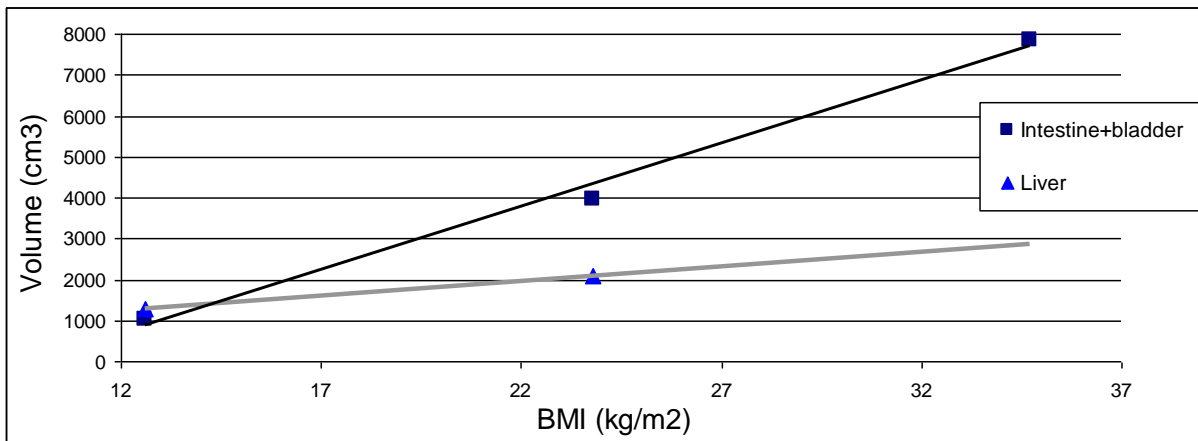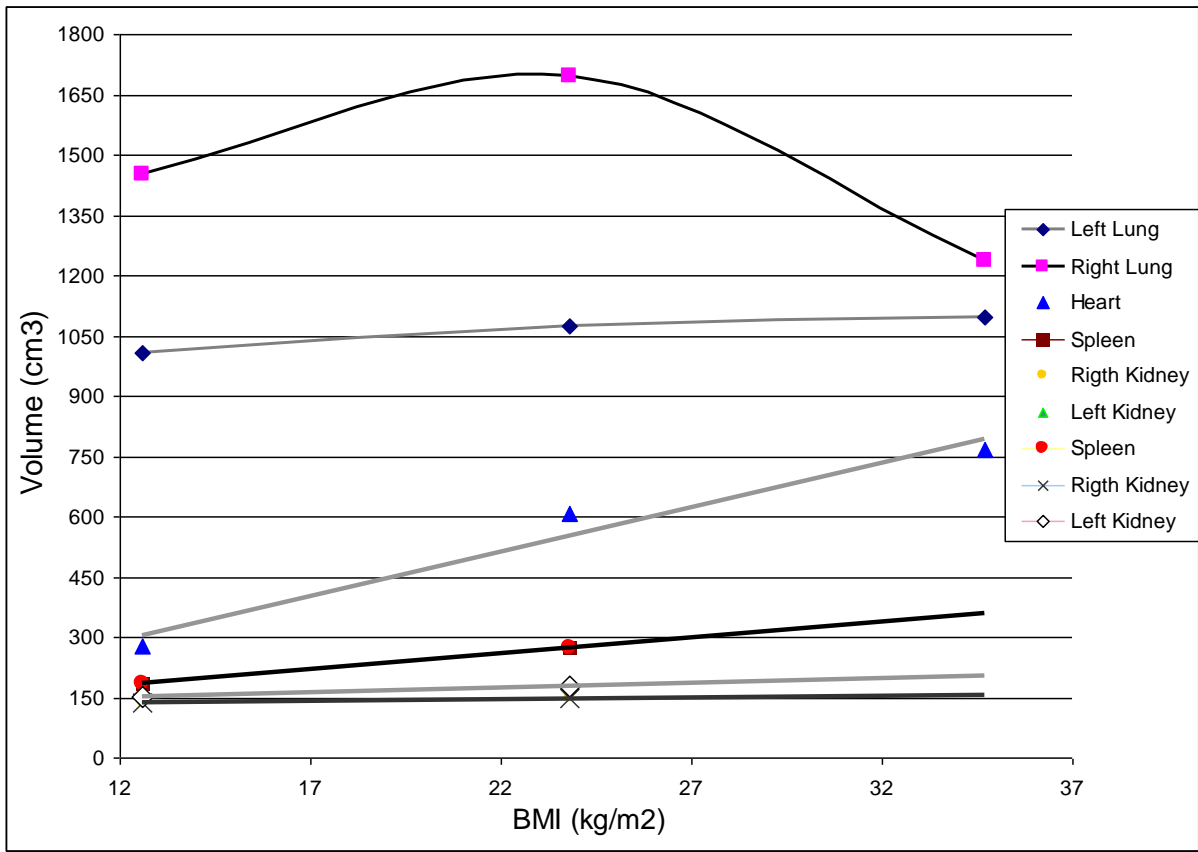
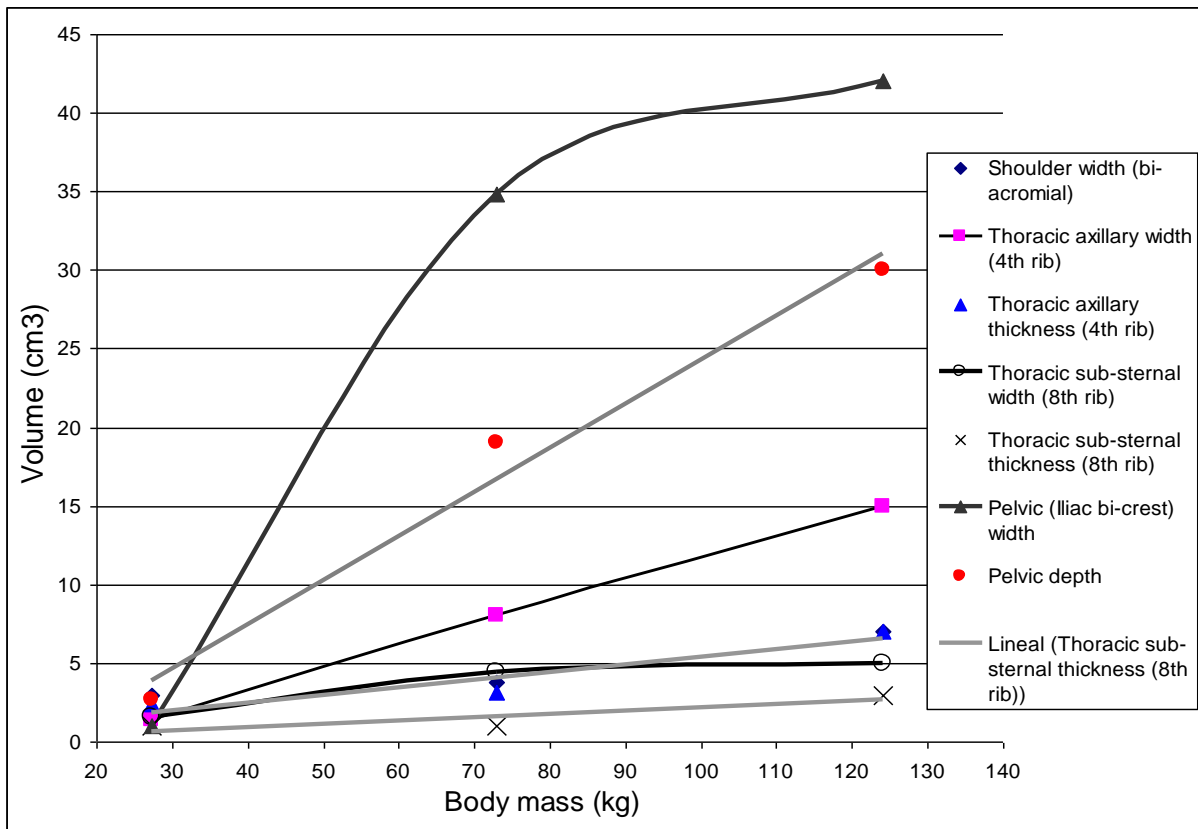*Figure 4.11: BMI versus volume internal organs of the three models*

Figure 4.12: Measure soft tissue versus body mass. Difference between measure taken excluding and including soft tissue.
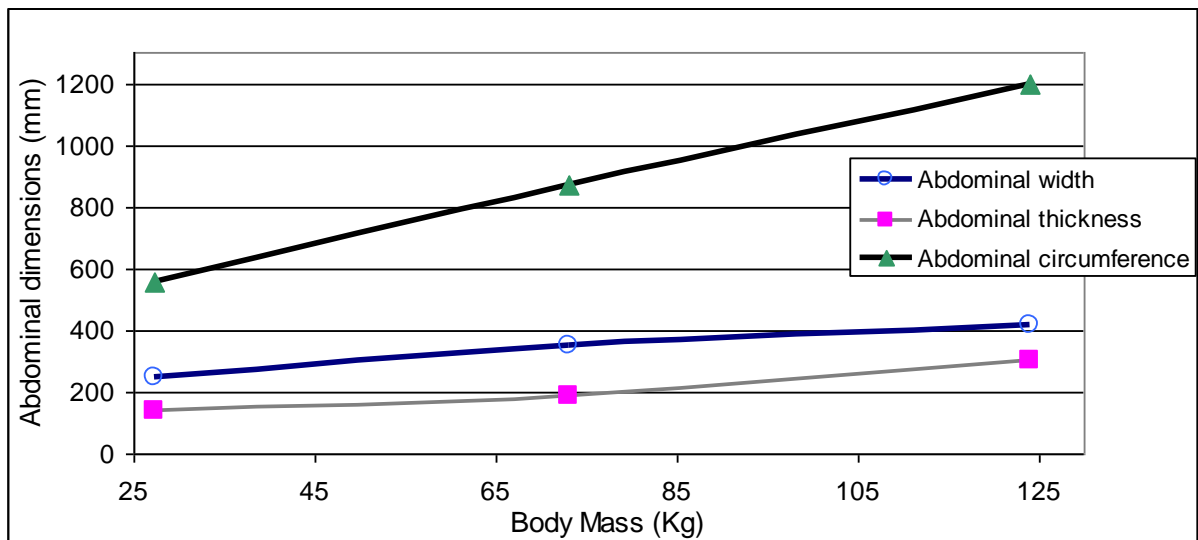

Figure 4.13: Body mass versus abdominal measure.

5 Discussion

In this section the results are analysed and compared to the information published in literature. A brief reviews of all aspects of the project is also given below.

5.1 Post mortem human subjects and software

The skeleton and skin were modelled in the three models, however some organs could not be modelled because of low quality data. The CT scan data has variation of quality. With low quality 12th rib was missed and there was a fusion of the first and second rib. In addition, some ribs lose the smooth shape.

For processing of data, four software (3D Slicer, Mimics, Amira and Simpleware) were selected and evaluated. 3D Slicer could not model any organ successfully. Mimics, Amira and Simpleware were available to use with the data. The main difference between them is that graphical user interface. Therefore the time that the users has to spend processing the data and performing actions varies. To my experience, Amira was the software that was the fastest to get started with. Also, the software license cost varies. In this project Simpleware ScanIP/ScanFE was selected to create the mathematical 3D-surface models. Using Scan IP to segmentation of the images and to model, and Scan Fe to create, edit the mesh and export to finite element code.

Simpleware ScanIP/ScanFe was suitable for this project but has some limitation. The software has a restriction to open files, limited memory of data. This is not tested for Mimics and Amira. It can be solved by cropping the image and get rid of unnecessary areas. In addition, the number and size of elements of the mesh cannot be defined in Simpleware ScanIP/ScanFE, but the size of the mesh elements can be reduced. In Mimics and Amira the number and size of elements can be defined.

The software LS-PrePost was chosen to assemble the models. The assemble could have been done with Simpleware. In my opinion, it would be faster to create individual models with Simpleware and assembly with LS-PrePost.

5.2 Models

The main anthropometry dimensions of the models are extracted and compared with the data of the subjects. Three dimensions human shape analysis is large number of measured points. By choosing of the dimensional measures the results can be different. The data extracted of the subjects is relative; the three models are not aligned and have a small rotation in the "z" axis (longitudinal axis of the model). The results of the anthropometric dimensions of the models are close to the measure was taken from the subjects.

The measure of abdominal in direction width in the model F437 extracted from the report NHTSA (Forman J., Lessley D., Kent R. 2009) can be not correct. The measure extracted by the University of Virginia from the subject was 94.5 cm. According with the others measures and the measure taken from the model, it can be 24.5 cm.

For this study, two men and a woman were analysed but the dimensional anthropometrics men and women differ in their bodily composition. The fat is distributed differently, in general women having a propensity to accumulate fat in the thorax, pelvis and below the

umbilicus instead in men, abdominal fat accumulate above the umbilicus (Pheasant, S., Haslegrave, CM.. (2006)). But in this project the difference between male and female cannot be evaluated, more data would be needed.

The anthropometric measures are taken including and excluding soft tissue, so the dimension of the layer of the skin and fat layer can be extracted. Studying the result of these three subjects, the thickness of the soft tissue has increased proportional to the increase of the body mass. This increase is higher in the pelvis area than the thoracic, especially in the thoracic sub external (8th rib) is very small. In which, both curves (width and thickness) have almost the same slope so the soft tissue is distributed uniformly in this area.

It is not the same for the thoracic axillaries (4th rib) area where the increase is greater in the width measure than the thickness. In this case the soft tissue is not distributed uniformly. As body mass increases, mass soft tissue is accumulating in the width direction than in the thickness. The ratio of nearly twice respect increase of the measure in the width than thickness direction, although these values can depend on the position of the subject. The subjects are in supine posture when the scanner was making. The internal organ and soft tissue measures can depend on the posture so the subject. In addition, the increase of the measure of the soft tissue is higher in direction width than depth of the pelvis. So the soft tissue is distributed uniformly, more pronounced abdominal and pelvis than thorax. The external measures of the skin of the abdominal increase lineally with the body mass. In the both direction: thickness and width increase proportionally, have similar slope.

The measure anthropometry are comparing with the size internal organs, excluding aorta. About the volume of right lung is higher than left caused to the space occupied by the heart. Otherwise the volume of the left kidney is higher than the right, around ten percent. And the right kidney is slightly lower than the left, because the situation of the liver besides volume of right kidney shows an increase greater than left kidney comparing with the body mass, height or sitting height. The measure of the volume of the right lung decreases. It can be caused by the lungs do not depends on anthropometric characteristics. It can depend others characteristics, as age or sex. Also, the lungs depends of the mass of the heart as it takes part of your space, especially the left lung. The lack of pressurization of the cadaver and its passive musculature, as it can induce a decrease the dimensions of some organs

The body mass, height and sitting height have a strong relationship with the size of the internal organs. Excluding the right lung, the correlation coefficients are very close than one, this means there is close than lineal relationship. The height is the characteristic strongest for the heart, lungs and intestine. The coefficient of correlation is only from the data of the organs: heart, left lung and intestine with bladder. The others organs cannot be taken into account (only two points).

The heart has a linear relation with the height; its correlation coefficient value is one. The heart also has a strong relation with the body mass and sitting height. The left lung and the intestine with bladder have a stronger relation with the height than the others anthropometric measures. And the intestine with bladder have strong relationship with sitting height, too. The greatest variation of this organs occurs when volume of them is compared with the height. The intestine shows big variation comparing with the body mass and the sitting height.

However for the liver, spleen and the kidneys have stronger relation with the sitting height, the greatest variation occurs when the volume of them is compared with the sitting height.

6 Conclusions

In this master thesis project three finite element meshes were developed, based on existing medical imaging techniques, such as CT scan data from three PHMS. These subjects were selected due to the various sizes and shapes. It could provide reconstructions of the upper body, external and internal geometric. To process the data, some software were evaluated and one was chosen. The software chosen was suitable, but has some limitation. The CT scan data was variation of quality, with low quality some ribs were missed and fusion. Although all bones and most of the organs were modelled.

In addition, the main anthropometric dimensions were extracted and the analyses anatomical done, to anthropometries the geometries of the upper body of the three human models. The external and internal measures were evaluated. Anthropometric and internal organs measure have a relationship close than the lineal relationship. And a large increase in the volume of the heart respect of the height and body mass. Otherwise, the lungs does not depend on the anthropometric measures. The distribution of the body mass is defined as higher increase of the soft tissue in the pelvis than in the thorax.

7 Future work

This analysis can use to scale the upper body of a human model. In addition, in the validity and of the mechanical response of the developed human finite elements models comparing with PHMS impact test data.

The models can be improved using CT scan data with higher resolution, or others medical techniques, as MRI.

The relation between internal organ size and external anthropometric measures can be improved using data from a larger number of specimens. Also, the models can be comparing data from the size of the organs between alive human and post mortem. And study the effects of posture on the position, shape and volume of the internal organs. In addition, male and female can be compared their anthropometric differences.

8 References

Aggarwal P., Sardana HK, Vig R. (2010): *An efficient visualization and segmentation of lung CT Scan images for early diagnosis of cancer*. National Conference on Computational Instrumentation. CSIO Chandigargh, India.

Azouz, ZB. et al. (2006): *Characterizing human shape variation using 3D anthropometric data*. Québec. Canada: Springer. Visual Computer, Vol 22, number 5, pp. 302-314.

Beillas P, Lafon Y, Smith FW. (2009): *The Effects of Posture and Subject-to-Subject Variations on the Position, Shape and Volume of Abdominal and Thoracic Organs*. University of Lyon, France: Stapp Car Crash Journal. Vol 53 (November 2009), pp.127-154.

Bertrand S. et al. (2008): *Three-dimensional reconstruction of the rib cage from biplanar radiography*. Laboratoire de biomécanique of Paris, France. IRBM Vol 29, Issue 4, Pages: 278–286.

Cahiill, Donald R. (1995): *Atlas of human coss-sectional anatomy:with CT abd MR Images*. 3rd edittion. New York : Ed. John Wiley & Sons, Inc.

Cornier J.M. (2008): *The Influence of Body Mass Index on Thoracic Injuries in Frontal Impacts*. Biodynamic Research Corporation, San Antonio, USA: Accident Analysis and prevention. Vol 40, issue 2, pp. 610-615.

Crandall, Jeff (2009): *Simulating the road forward: the role of computational modeling in realizing future opportunities in traffic safety*. International IRCOBI Conference on the Biomechanics of Impact. York, United Kingdom

Ellis H., Logan BM., Dixon A. (2007): *Human sectional anatomy: Atlas of body sections, CT and MRI images*. 3rd edition. London: Ed. Hodder Arnold.

Forman J., Lessley D., Kent R. (2008a): *NHTSA:Rear sear sled test report covering test 1332,1333,1334,1335*. Center for applied Biomechanics, University of Virginia. USA.

Forman J., Lessley D., Kent R. (2008b): *NHTSA:Rear sear sled test report covering test 1384,1385,1388*. Center for applied Biomechanics, University of Virginia. USA.

Forman J., Lessley D., Kent R. (2009): *NHTSA:Rear sear sled test report covering test 1386,1387,1389*. Center for applied Biomechanics, University of Virginia. USA.

Gayzik, F.; Moreno D.; Stitzel J. (2010): *The Development of Full Body Geometrical Data for Finite Element Models: A MultiModality Approach*. Winston-Salem, USA.

Grandmaison et al. (2001): *Human body size and the law of scaling: physiological, performance, growth, longevity and ecological ramifications*. New York: Nova science publishers, Inc.

Guide SlicerDicer (2010) PIXOTEC, LLC. Webpage <http://www.slicerdicer.com/> [Cited 16 April 2010].

Hansen JT., Netter FH. (2007): *Netter Anatomía. Fichas de autoevaluacion: Tronco*. 2th edition. New York : Ed. Elsevier-Masson..

Hernam, G. (2009): *Fundamentals of Computerized Tomography: Image Reconstruction from Projections*. London: Ed.Springer.

HFES 300 Committee (2004): *Guidelines for Using Anthropometric Data in Product Design. P*ublished by the Human Factors and Ergonomics Society. USA.

Hyung YC. et al. (2009): *Digital Elderly Human Body Modeling*. Presented at Digital Human Modeling for Design and Engineering Conference and Exhibition (June 2009), Gothenburg, Sweden.

Hyung YC. et al. (2009): *Elderly Human Body Modeling for Crash Safety Simulation*. Published by Dept. of Mechanical and System Design Eng., Hongik University, Seoul, and Korean Automobile Testing & Research Institute,Kyonggido, Korea.

Kai-Uwe Schmitt (2007): *Trauma Biomechanics: Accidental Injury in Traffic and Sports*. 2nd Edition. New York: Ed.Springer.

Klinich et al. (2008): *Abdominal Injury in Motor-Vehicle Crashes*. Transportation research institute, University of Michigan (UMTRI), USA.

Lav R. Varshney (2002) : *Abdominal Organs Segmentation in CT Scan Images*. A Survey. School of Electrical and Computer Engineering, Cornell University, Ithaca, New York. USA.

Lopez-Valdes F. et al. (2009): *A comparison beween a child-size PMHS and the hybrid III 6 YO in a sled frontal impact*.

Lopez-Valdes, F. et al. (2009): *The frontal-ompact response of a booster-seated child-size PMHS*. IRCOBI Conference-York, UK.

LS-Prepost Tutorial Guide (2010) Livermore Software Technology Corporation.USA < www.lstc.com> [Cited 1 September 2010]

Pheasant, S., Haslegrave, CM.. (2006): Body Space: Anthropometry, Ergonomics and the Design of Work. 3th edition. London: Ed. Taylor &Francis.

Scott Gayzik, F. (2009*): A Multi-Modality Image Data Collection Protocol for Full Body Finite Element Model Development*. Presented at SAE World Congress & Exhibition (April 2010), Detroit, USA.

Serre T. (2002): *The seated man: geometry acquisition and three-dimensional reconstruction*. Marseille. France: Ed.Springer. Surgical and Radiologic Anatomy, vol. 24, number 6, pp.381-186.

Shigeta K., Kitagawa Y, Yasuki T. (2009): *Development of next generation human FE model capable of organ injury prediction.* Paper number 09-0111, Toyota Motor Corporation, Japan

Simleware Tutorial Guide (2010) SIMPLEWARE LTD Innovation centre rennes drive. Exeter, United Kingdom. Webpage <http://www.simpleware.com/>[Cited 1September 2010].

Simpleware Reference Guide (2010) SIMPLEWARE LTD Innovation centre rennes drive. Exeter, United Kingdom. Webpage <http://www.simpleware.com/> [Cited 1 September 2010].

Tortora, GJ.; Derrickson, B. (2005): *Introduction to Human Body: The essential of Anatomy and Physiology*. 7 Th edition. New York, USA: Ed. John Wiley & Sons, Inc.

Tutorial Guide AMIRA (2010) AMIRA, Ltd. Webpage. <http://www.amira.com/> [Cited 30 April 2010].

Tutorial Guide IA-FEMesh. The University of Iowa: IA-FEMesh. Iowa, United States. Webpage. <http://www.ccad.uiowa.edu/mimx/IA-FEMesh/> [Cited 16 April 2010].

Tutorial Guide Materialise: MIMICS (2010), Materialize Inc, webpage. <http://www.materialise.com/> [Cited 30 April 2010].

Tutorial Guide of 3D Slicer(2010) Webpage <http://www.slicer.org/> [Cited 30 April 2010].

Tutorial Guide of FreeSurfer. Athinoula A.Martinos Center for Biomedical Imaging. Webpage <http://surfer.nmr.mgh.harvard.edu/> [Cited 16 April 2010].

Tutorial Guide of GemIdent (2006) University of Stanford. Webpage <http://gemident.com/> [Cited 16 April 2010].

Tutorial Guide of ImageJ. Research Service Branch, Maryland, USA. Webpage <http://rsb.info.nih.gov/ij/>[Cited 16 April 2010].

Tutorial Guide of ITK –VTK. Kitware, Inc. USA. Webpage<http://www.vtk.org/> [Cited 16 April 2010].

Tutorial Guide of MicroDicom. NEMA. Webpage <http://www.microdicom.com/> [Cited 16 April 2010].

Viano, D., Parenteau, C. (2008): *Crash Injury Risks for Obese Occupants*. Detroit, USA: ProBiomechanics LLC. Presented at SAE World Congress & Exhibition (April 2008)

Young et al. (2008): *An efficient approach to converting three-dimensional image data into highly accurate computational models*. School of Engineering, Computing and Mathematics, University of Exeter. Exeter, UK: Philosophical Transactions of Royal Society A, vol 366, issue 1878, pp. 3155-3173.